

# In Silico Studies on HIV-1 Integrase Inhibitors: A Review

Basheerulla Shaik

# In Silico Studies on HIV-1 Integrase Inhibitors: A Review

## ABOUT THE AUTHOR

**Satya P Gupta<sup>1</sup>, Basheerulla Shaik<sup>1\*</sup>, Izhar Ahmad  
and Vijay K Agrawal<sup>2</sup>**

<sup>1</sup>Department of Applied Sciences, National Institute of  
Technical Teachers' Training, India

<sup>2</sup>Department of Chemistry, APS University, India

## CORRESPONDING AUTHOR

Basheerulla Shaik, Department of Applied Sciences,  
National Institute of Technical Teachers' Training,  
Bhopal-462002, India,

**Email:** [basheerulla.81@gmail.com](mailto:basheerulla.81@gmail.com)

**Published By:**

**MedCrave Group LLC**

October 31, 2016

<b>Abstract</b>	1
<b>Introduction</b>	2
<b>HIV-1 Integrase</b>	2
<b>Integrase Inhibitors</b>	2
Oligonucleotides	2
Curcumin analogues	3
Polyhydroxylated aromatic compounds	3
Diketo acids	4
Caffeol-based inhibitors	4
Hydrazides and amides	5
Tetracyclines	5
Deposides and depsidones	5
Chalcones	5
Miscellaneous	5
<b>Quantitative Structure-Activity Relationship (QSAR) Studies</b>	5
Polyhydroxylated aromatic compounds	7
Chalcones	9
Amides, Sulfonamides and Phthalamides	10
Carboxylic acid derivatives	15
Hydrazides	15
Curcumins	17
$\beta$ -Diketoacids (BDKAs)	19
Structurally different classes of compounds	21
<b>An Overall View</b>	25
<b>References</b>	25

## Abstract

Acquired immunodeficiency syndrome (AIDS) is a formidable pandemic that is still creating havoc world-wide. The curative agent of this disease has been found to be a virus called human immunodeficiency virus of type-1 (HIV-1). In the replicative cycle of HIV-1, the integration of the viral DNA into host chromosomes is an essential step that is catalyzed by the enzyme integrase (IN). Inhibition of this enzyme, therefore, provides an attractive strategy for antiviral drug development. Since integrase has no known structural analogue in human cells, it has been found to be a safer target than other targets to develop anti-HIV drugs. Several classes of compounds, such as oligonucleotides, curcumin analogues, polyhydroxylated aromatic compounds, hydrazides, amides, diketoacids, chalcones, etc., have been studied for HIV-1 integrase inhibition activity. To design and develop potent and effective IN inhibitors, several authors made quantitative structure-activity relationship (QSAR) studies on many classes of these IN inhibitors in order to provide the rationale for designing more potent drugs. This article presents a comprehensive, critical review on all QSAR studies reported so far in order to present an overall view on drug-receptor interaction and the important physicochemical properties of the molecules that govern their HIV-1 IN inhibition activity.

## Introduction

Today it is well known that acquired immunodeficiency syndrome (AIDS) is a fatal disease, which is caused by a virus called human immunodeficiency virus of type-1 (HIV-1). The HIV-1 is an enveloped virus of about 100 nm diameter [1] that consists of two major viral glycoprotein, the external gp120 and the transmembrane gp41 (gp stands for glycoprotein and the number refers to the mass of protein in thousands of Dalton). The HIV life cycle begins with high affinity binding of gp120 envelope to its receptor CD4 present on the surface of the host cell [2]. The replicative cycle of HIV-1 involves several steps, among which the most important are the viral binding to target cells, virus cell fusion, virus uncoating, reverse transcription of genomic RNA, viral integration, gene expression, cleavage event, and virion maturation. By hitting any of these stages, the viral replication can be terminated [3].

In the recent past, however, the attention was mostly focused on the inhibition of reverse transcription of genomic RNA and the cleavage event, for which variety of reverse transcriptase (RT) inhibitors [4] and HIV-1 protease inhibitors [5,6], respectively, were developed, and in abundance are available structure-activity relationship studies on them [7,8]. However, because of development of resistance in virus against RT and protease inhibitors, the chemists focused their attention on the third most important step in the life cycle of virus, the viral integration [9]. To hit the viral integration, the study on integrase inhibitors was started.

## HIV-1 Integrase

The integration of viral DNA into the host cell genome is translated as the basis of life-long infection. This biochemical event is catalyzed by the enzyme integrase and thus the study of integrase inhibition has drawn great attention of chemists.

The viral integration by integrase involves both *in vivo* and *in vitro* three steps [10-12]: (1) 3'- end processing reaction in which two nucleotides (GT) from the 3'- ends of each strand of linear viral DNA are removed by the enzyme, leaving at the viral 3'-ends the conserved CA dinucleotide, (2) strand transfer (ST) reaction, in which the enzyme makes staggered cuts in the target DNA and ligates the recessed 3'-OH ends of the viral DNA at the cleavage site, and (3) 5'- end joining reaction that leads to the completion of the

integration process, removing two unpaired nucleotides at the 5'-ends of the viral DNA and repairing the gaps between the viral and target DNA sequences. Out of these three steps, the first two represent a trans-etherification reaction, requiring the presence of divalent cations,  $Mn^{2+}$  and  $Mg^{2+}$ . This reaction is brought about by a direct nucleophilic attack on an internucleotide phosphate by the hydroxy group.

## Integrase Inhibitors

A number of structurally different classes of compounds have been found to act as integrase inhibitors. Due to a nonspecific interaction with the DNA binding domain of the enzyme, several DNA binding agents were found to inhibit HIV-1 integrase [13]. However, varieties of other groups of compounds as mentioned below have been studied for integrase inhibition [9].

- Oligonucleotides
- Curcumin Analogues
- Polyhydroxylated Aromatic Compounds
- Diketo Acids
- Caffeol-based Inhibitors
- Hydrazides and Amides
- Tetracyclines
- Depsides and Depsidones
- Chalcones
- Miscellaneous

A structural description of these compounds are given below

### Oligonucleotides

Some representative structures of oligonucleotides may be as shown in Figure 1, where  $R=5'$ -GTGTGGAAAATCTCAGC and 'A' may be H or GT. If  $R^1=H$ , it is called 19-mer oligonucleotides, and if  $R^1 = GT$ , it is called 21-mer oligonucleotides. The 19-mer oligonucleotides, with modifications of 3'-OH, were found to significantly reduce the strand transfer reaction, while 21-mer oligonucleotides were found not only to competitively inhibit strand transfer (ST) reaction but also 3'-processing (3'-P) reaction with nanomolar  $IC_{50}$  values [14].

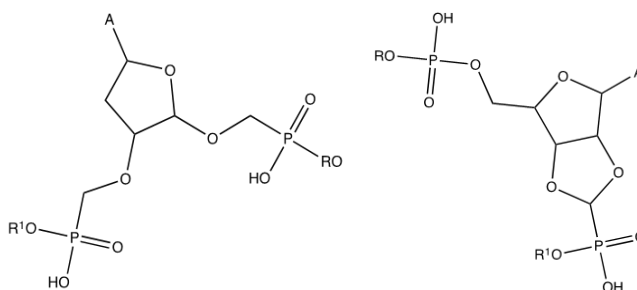


Figure 1: Some representative structures of oligonucleotides.

### Curcumin analogues

Curcumin analogues have the general structure as shown in Figure 2. Curcumin belongs to the family of curcuminoids (phenolic diarylheptanoids), which are characteristic, yellow coloring constituents of turmeric. It is diferuloylmethane and it has been reported to inhibit both 3'- processing and strand transfer reactions with  $IC_{50}$  values equal to 150 and 140  $\mu$ M, respectively [15]. Analogues of curcumin were found to bind in the enzyme catalytic core [16]. The catalytic core domain of HIV-1 integrase contains the invariant triad of acidic residues, the D, D-35-E motif [17-20], comprising of residues Asp64, Asp116, and Glu152. These catalytic residues are in close proximity, coordinate with divalent metal ions and define the active site.

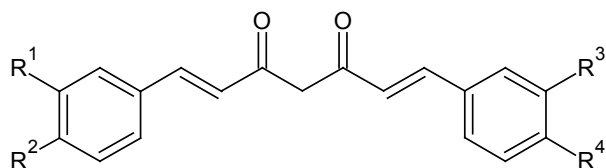


Figure 2: General structure of curcumin analogues.

### Polyhydroxylated aromatic compounds

Polyhydroxylated aromatic compounds such as shown in Figure 3 were found to lead to potent integrase inhibitors [21-23]. Structures containing catechol or bis-catechol, such as Figure 3e & Figure 3f, were however most extensively studied [16,23-30]. A bis-catechol derivative, L- chicoric acid (Figure 3g) and a polyhydroxylated compound devoid of catechol moiety, aurintricarboxylic acid (ATC, Figure 3h), were found to have high integrase inhibition activity [31].

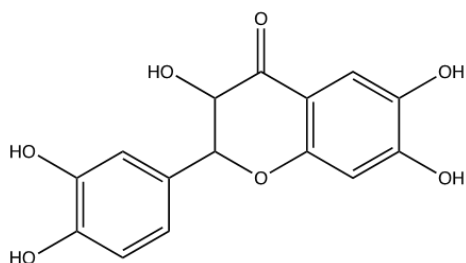


Figure 3a: (quercetin)

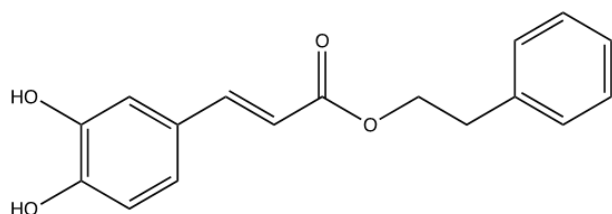


Figure 3b: (CAPE)

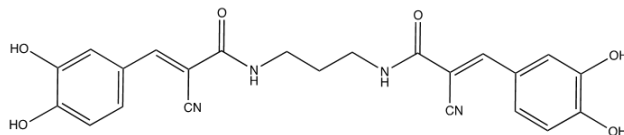


Figure 3c: (a tyrphostin).

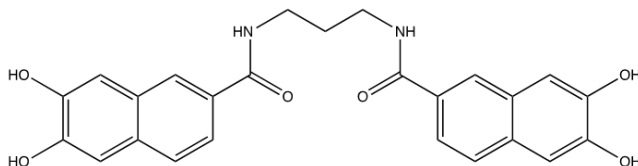


Figure 3d

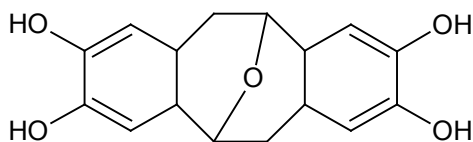


Figure 3e

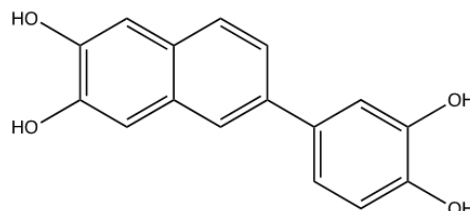


Figure 3f

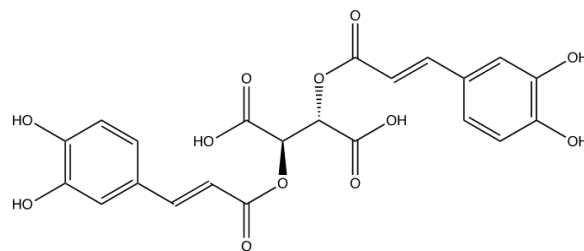


Figure 3g

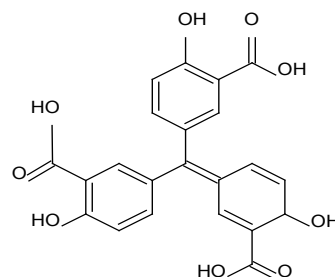


Figure 3h

Figure 3: Examples of some polyhydroxylated aromatic compounds.

## Diketo acids

Another emerging class of integrase inhibitors is related to aryl  $\beta$ -diketo (ADK) based agents with general structure as shown by Figure 4a. The best two examples of ADK-based inhibitors are L-708, 906 (Figure 4b) [32] and 5CITEP [1-(5-chloroindol-3-yl)-3-hydroxy-3-(2H-tetrazo-5-

yl)-propenone] (Figure 4c) [33]. Same authors found that a variety of substituent on the left side aryl ring of 'a' were able to maintain the good strand transfer inhibitory potency, but the carboxylic acid containing substituent were good to enhance 3'- processing inhibitory potency, reducing selectivity towards strand transfer reactions.

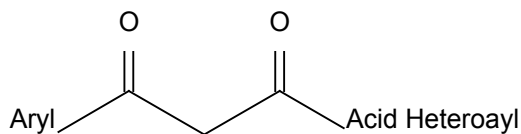


Figure 4a

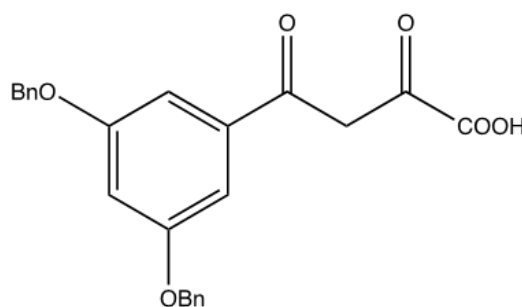


Figure 4b

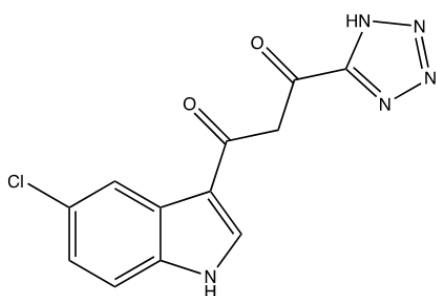


Figure 4c: (5CITEP)

Figure 4: Some examples of aryl  $\beta$ -diketo (ADK) based agents where 'a' represents the general structure.

## Caffeoyl-based inhibitors

Caffeoyl-based inhibitors are caffeic acid esters separated by aliphatic, alicyclic, or aromatic linkers [25,34] (Figure

5). In Figure 5, 'a' represents a caffeoyl-based integrase inhibitor and 'b' a caffeoyl unit.

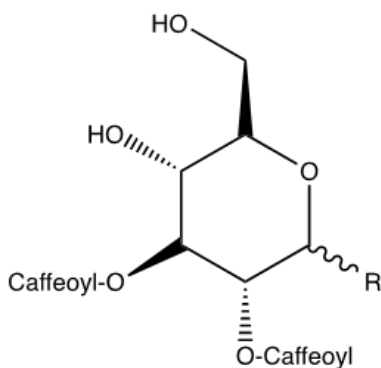


Figure 5a

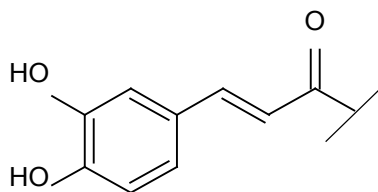


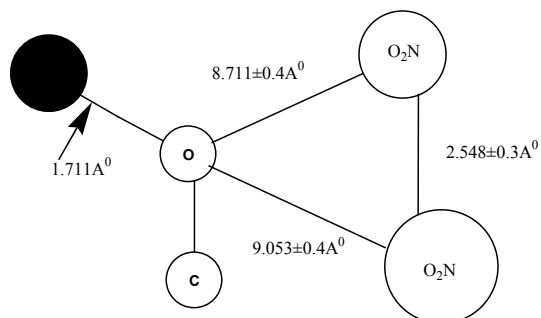
Figure 5b

Figure 5: Caffeoyl-based integrase inhibitors.

## Hydrazides and amides

A pharmacophore derived by Nicklaus et al. [35] on the basis of certain potent integrase inhibitors was proposed to have three hydrogen-bond (H-bond) acceptor atoms

that could also form complexes with the positively charged ions (Figure 6). On the basis of this pharmacophore, some hydrazides, as represented by Figure 7, were developed and found to possess good integrase inhibition activity [36].



**Figure 6:** A pharmacophore model as suggested by Nicklaus et al. [35] for HIV-1 integrase binding. The shaded sphere is an (steric) exclusion sphere.

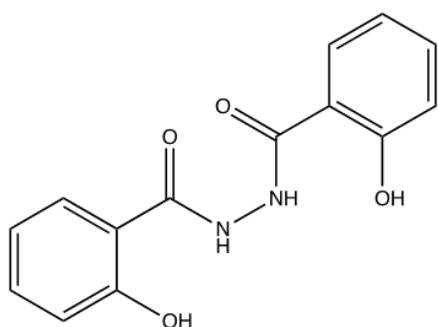


**Figure 7a**

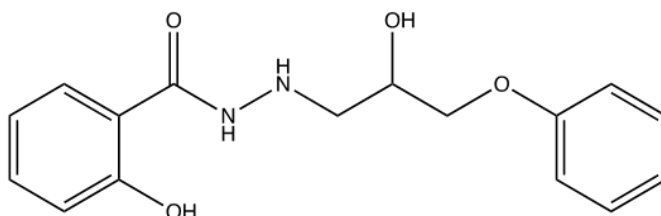


**Figure 7b**

**Figure 7:** Structures of some hydrazides developed, based on the pharmacophore model as shown in Figure 6

In polyamide series, some bisdistamycin and lexitropsin derivatives such as those shown in Figure 8, where X may be a distamycin or a lexitropsin moiety, were developed [37]. A small series of netropsin derivatives such as those shown in Figure 9 were also developed [37]. All distamycin, lexitropsin, and netropsin derivatives were found to act as integrase inhibitors, but to have more potency in the presence of  $Mg^{2+}$  ions than in the presence of  $Mn^{2+}$  ions.

## Tetracyclines

Neamati et al. [38] also studied the integrase inhibition activity of tetracyclines (Figure 10). A series of tetracyclines were studied in the presence of both  $Mn^{2+}$  and  $Mg^{2+}$  ions to find that there was little difference in their potency in either ion.

## Depsides and depsidones

A depside is a type of polyphenolic compound composed of two or monocyclic aromatic units such as shown by Figure

11a and a depsidone is a compound that consists of esters but also is cyclic ether (Figure 11b). Neamati et al. [39] also studied a series of depsides and depsidones for their integrase inhibition activity and found certain compounds to possess very high potency having  $IC_{50}$  values around  $1\mu M$

## Chalcones

A chalcone (Figure 12) is aromatic amine and andenone that forms the central core for a variety of important biological compounds. They are collectively called as chalcones and chalconoids. Chalcones may also be called as phenyl styryl ketones. Chalcones have also been studied by some authors as HIV-1 integrase inhibitors [40].

**Miscellaneous** In addition to above mentioned classes, some sulfonamides [41,42], quinolone carboxylic acids [43], isoquinolines [44], styrylquinolines [45,46], phthalimides [47], etc., have also been studied for HIV-1 integrase inhibition.

Quantitative Structure-Activity Relationship (QSAR) Studies

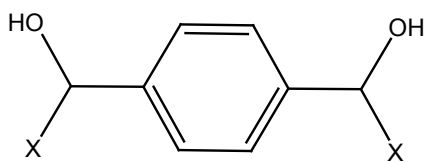


Figure 8a

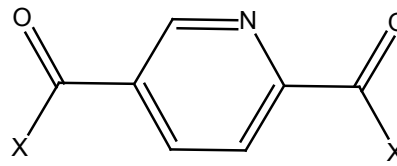
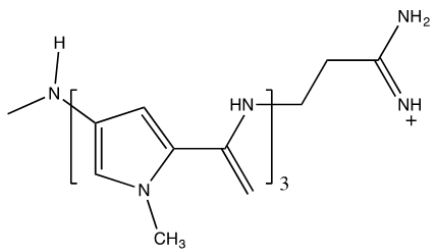
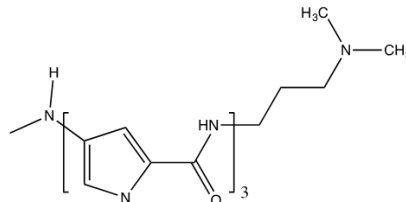


Figure 8b



Dist moiety



Lexitropsin moiety

Figure 8: Examples of some bisdistamycin and lexitropsin derivatives

Net-CO (CH<sub>2</sub>)<sub>n</sub> CO-Net  
Figure 9a



Figure 9b

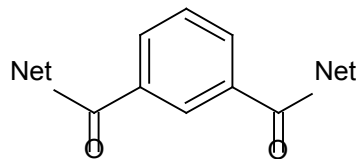
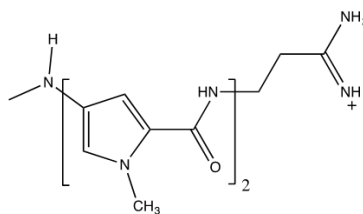


Figure 9c



Netropsin moiety

Figure 9: Examples of some netropsin derivatives.

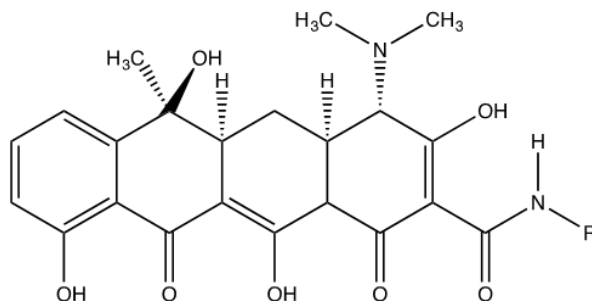


Figure 10: Structures of Tetracycline.

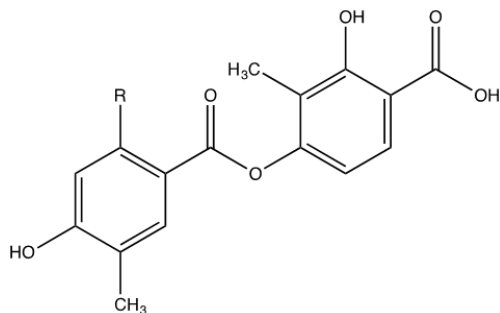


Figure 11a

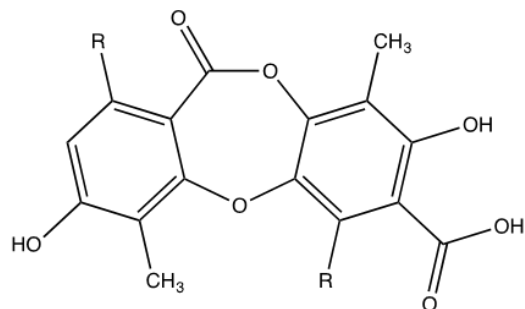


Figure 11b

Figure 11: Structures of depsides (a) and a depsidones (b).

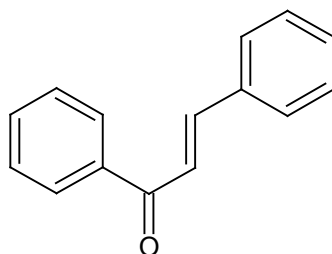


Figure 12: Structure of a chalcone.

For many of the above mentioned classes of integrase inhibitors, some QSAR studies have been made in order to find their physicochemical and structural properties that govern their activity and to have an idea as to how they interact with the receptors. Such studies provide the rationale to modify structures of the drugs so that highly potent and less toxic drugs can be obtained. Now we present here all the QSAR studies available on integrase inhibitors and discuss their implications. These QSAR studies include all possible approaches such as Hansch type analysis, Comparative Molecular Field Analysis (CoMFA), Comparative Molecular Similarity Analysis (CoMSIA), pharmacophore mapping, docking, etc.

### Polyhydroxylated aromatic compounds

A large number of potent HIV-1 integrase inhibitors have been found to have in common two aryl units separated by a central linker, where one of these aryl moieties must contain 1, 2-dihydroxy substituents. The requirement of hydroxyl groups led many authors to study polyhydroxylated compounds and perform QSAR studies.

A series of cinnamoyl analogues, with a representative structure as shown in Figure 13, was subjected to QSAR studies by Boulamwini & Assefa [48]. The HIV-1 integrase inhibition data of these compounds were taken from Artico

et al. [49]. CoMFA and CoMSIA studies and docking simulations were conducted on these compounds. From the CoMFA study, the favorable steric and electrostatic regions were indicated. The two regions flanking the carbonyl or keto-enol moiety of the compounds were suggested to be sterically unfavorable. The regions close to oxygen atoms of the catechol moieties were suggested to be favorable for electronegative groups, which is consistent with the observation that polyhydroxylation generally enhances integrase inhibitory activity [50].

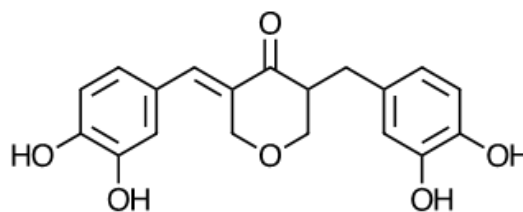
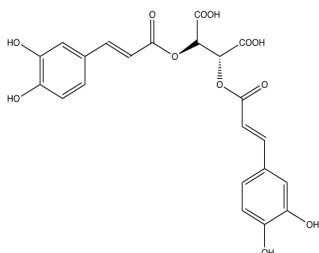


Figure 13: A representative structure of cinnamoyl analogues.

In CoMSIA studies the hydrophobic and hydrogen-bond donor and acceptor fields are also indicated, in addition to electrostatic and steric fields. The CoMSIA electrostatic and steric fields were similar to those of CoMFA. In CoMSIA

studies the H-bond donor fields were found to make the greatest contribution, which was strongly supported by FlexX docking results. The regions where hydrophobicity was favored were found to occur over the receptor surface of moderate hydrophobic potential and the regions where hydrophobicity was disfavored were shown in the proximity to polar keto-enol moiety, which interacts with hydrophilic amino acid residues. The integrase active site has been found to accommodate large variations in ligand size and shape and different binding modes.

For a series of chicoric acid derivatives, with the representative structure as shown in Figure 14, that are also polyhydroxylated aromatic compounds, Sahu et al. [51] made a simple QSAR study for their 3'-processing as well as overall integration inhibition activities that were reported by Xu et al. [52]. The QSAR models obtained were as follows.



**Figure 14:** A representative structure of chicoric acid.

### 3'-processing inhibition

$$\log(1/IC_{50}) = 15.383(\pm 2.470) - 0.026(\pm 0.003)HF + 14.782(\pm 2.060)E_{LUMO} - 0.528(\pm 0.315)\log P - 0.021(\pm 0.003)SAS$$

$$n = 19, r = 0.925, r^2_{cv} = 0.781, s = 0.399, F = 17.94 \quad (1)$$

### Integrase inhibition

$$\log(1/IC_{50}) = 19.716(\pm 3.246) - 0.025(\pm 0.004)HF + 17.814(\pm 2.737)E_{LUMO} - 0.882(\pm 0.192)\log P - 0.336(\pm 0.051)BK01$$

$$n = 20, r = 0.880, r^2_{cv} = 0.620, s = 0.494, F = 12.83 \quad (2)$$

In these equations, HF refers to heat of formation,  $E_{LUMO}$  stands for the energy of the lowest unoccupied molecular orbital,  $\log P$  is the hydrophobicity of the molecule, SAS denotes the solvent accessible surface area, and BK01 is the basic kappa of order 1. Among the statistical parameters,  $n$  is the number of data points,  $r$  is the correlation coefficient,  $r^2_{cv}$  is the squared correlation coefficient obtained by leave-one-out jackknife procedure,  $s$  is the standard deviation,  $F$  is the  $F$ -ratio between the variances of calculated and observed activities, and the data within the parenthesis with  $\pm$  sign are 95% confidence intervals. From the values of these statistical parameters, both the models were found to be quite significant, indicating that both the 3'-processing and integration inhibitory activities of the compounds were commonly governed by the heat of formation, hydrophobicity, and the energy of the highest occupied molecular orbital of the compounds. However, while for both the activities the heat of formation and hydrophobicity were conducive

only at low values, the energy of the lowest unoccupied molecular orbital was conducive at high value. The  $E_{LUMO}$  refers to the electron affinity of the molecule and thus the involvement of electron affinity of the molecule might indicate the involvement of charge-transfer phenomenon in drug receptor interaction.

In eq. (1), the negative coefficient of SAS indicated the requirement of low value of solvent accessible surface area for better 3'-processing inhibitory activity, while in eq.(2) the negative coefficient of BK01 indicated the requirement of low value of basic kappa of order 1 for better integration inhibitory activity. In fact, both SAS and BK01 indicate the steric effects.

For the two different sets of compounds, one comprising of catechols and one non-catechols, Makhija & Kulkarni [53] made a QSAR study using genetic function approximation (GFA). GFA generates a population of equations rather than one single equation for correlation between biological activity and physicochemical parameters. By examining different models generated by GFA, additional information can be discerned. The frequency of occurrence of particular descriptors in the population indicates its relevance. From their GFA analysis, Makhija and Kulkarni found that for non-catechols the 3'-processing inhibition was largely controlled by spatial, thermodynamic and shape descriptors, while 3'-strand transfer inhibition was also affected by H-bond donor groups in addition to spatial and thermodynamic parameters. In case of catechols, both 3'-processing and 3'-strand transfer inhibition activities were found to be controlled by some electronic descriptors, shape related physicochemical parameters, and some thermodynamic descriptors related to desolvation phenomena during binding.

For a fairly large series of styrylquinolines studied for their HIV-1 integrase inhibition activity by Mekouar et al. [45] and by Zouhri et al. [46], Ma et al. [54] performed CoMFA and docking studies in order to explore the mode of binding of these compounds with the enzyme. These compounds also belong to the group of polyhydroxylated aromatic compounds. A representative member of this series may be such as shown in Figure 15. For both CoMFA and docking studies this compound was used as a template. A good CoMFA model was derived that could accurately predict the activity of test set compounds. CoMFA contour maps were drawn for showing the steric, electrostatic and H-binding features. In the steric and electrostatic maps, the presence of a bulky group near the carboxylic group at C-7 was suggested to be favorable and near C-8 unfavorable. Similarly, a positive charge near the H-atom of carboxylic group, N-1 and C-3' was suggested to be conducive. On the other hand, a negative charge was found to be conducive near the carboxylic oxygen atom of C-7.

In the contour plot of H-bonding, the H-bond acceptor groups near the OH of C-4' and that of C-7 carboxylic group were indicated to be favorable and an H-bond donor was shown to be favorable near N-1.

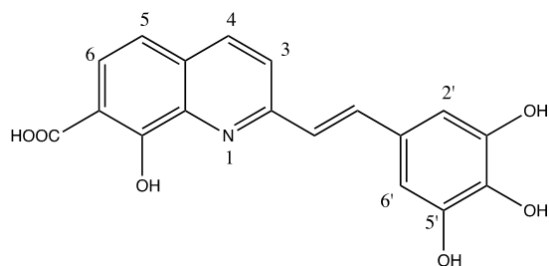
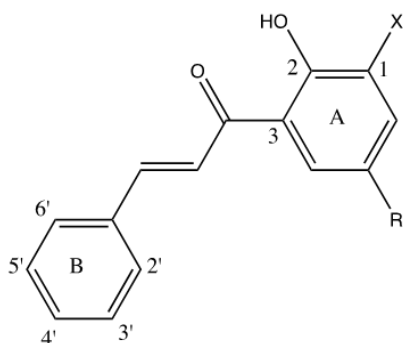


**Figure 15:** A representative structure of styrylquinolines.

The well-clustered docking results were obtained for most of the investigated styrylquinolines to observe two clusters, occupying two separate but overlapping binding regions. The two clusters occupy a narrow binding region formed by Asp64, Ser66, Leu68, Gly70, Asp116, Gln148, Gly149, Glu152, Asn155, Lys156 and Lys159. Also the oxygen atoms of C-7 carboxylic group and C-8 hydroxyl group were shown to coordinate with  $Mg^{2+}$  within the enzyme catalytic site.

### Chalcones

A series of chalcones with general structure as shown in Figure 16 was studied by Sharma et al. [55] for HIV-1 integrase inhibitory activities (3'-processing as well as 3'-strand transfer). Since no crystal structure of human integrase-ligand-DNA complex is available, these authors first developed a pharmacophore model using PHASE program. The three most potent compounds of the series, a, b and c, were selected as actives for use in identifying a common pharmacophore. The pharmacophoric features as shown in Figure 17 were two H-bond acceptor groups (A), two hydrophobic groups (H), a negative feature (N) and an aromatic ring (R). This pharmacophore was mapped onto the compound b.



a: 4'- Br; X= COOH, R= Br

b: 2', 4'-diCl; X= COOH; R =Br

c: 2',3',6'-tri Cl; X= COOH; R= Br

**Figure 16:** General structure of chalcones.

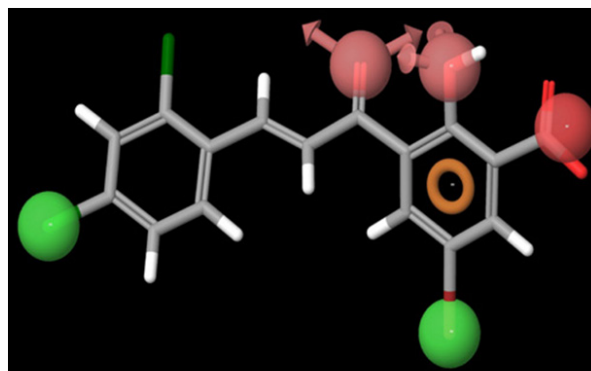


**Figure 17:** The best pharmacophore hypothesis (AAHNR) mapped onto compound b (Figure 16). Pharmacophore features are: red spheres and vectors for H-bond acceptor (A), brown rings for aromatic groups (R), dark red spheres refer to a negative feature (N) and green spheres indicate hydrophobic groups (H). Atoms in the ligands are represented as: O by red; Br by wine red; Cl, by dark green; H by white, C by gray.

Through CoMFA and CoMSIA studies, Sharma et al. tried to find the favorable and unfavorable regions for steric, electrostatic, hydrophobic, H-bond acceptor and donor interactions. As shown in Figure 18, the steric CoMFA maps (Figure 18a) had indicated, through green contours around the ortho and para positions on aryl ring B, that bulky groups would be favored at these positions. A large yellow contour surrounding a small green contour at Meta position on aryl ring B suggested that only a limited bulk would be favored at this position. The CoMFA electrostatic map (Figure 18a) revealed a red contour at the 3'-position suggesting that electronegative groups at this position could increase the activity. The distant blue contours around aryl ring B indicated that electropositive groups should increase activity at these positions.

The CoMSIA steric and electrostatic maps (Figure 18b) were almost similar to those of CoMFA. However, the hydrophobic, H-bond donor and acceptor contour maps of CoMSIA (Figure 18c) indicated that a white contour located near the R-substituent and two more such contours at 2' and 5'-positions of the B ring may be the regions where hydrophilic groups might favor the activity. Another white contour at the 3-keto oxygen also indicated a favorable region for the hydrophilic group. The only favorable position for a hydrophobic substituent was indicated by a yellow contour close to 4'-position on ring B. The magenta contour at 3-keto functionality suggested that this oxygen would act as H-bond acceptor. A cyan contour appearing close to and merging into a magenta contour suggested that 2-OH would act as H-bond donor that might be involved in H-bond interactions with the acceptor carboxylate groups of the acidic catalytic triad residues of integrase active site

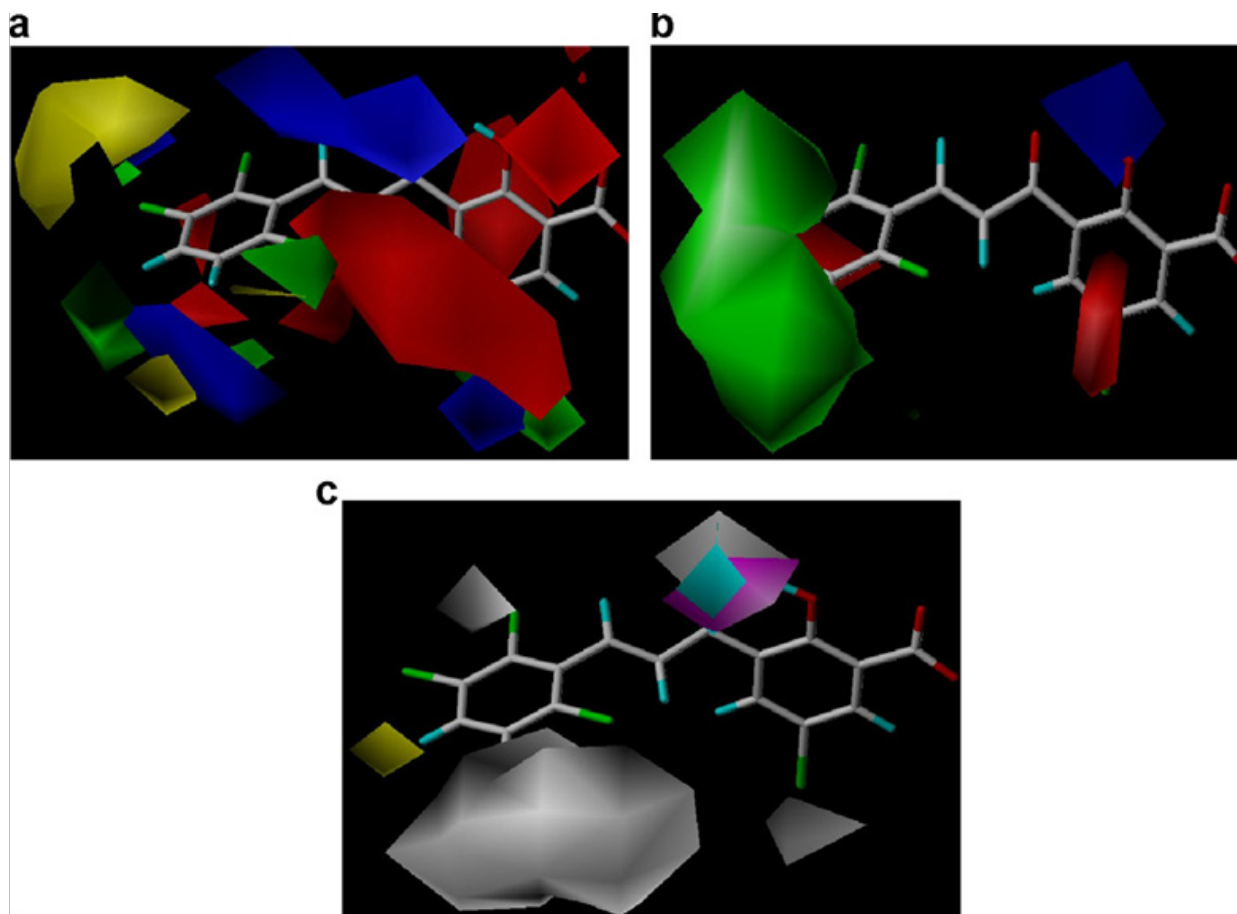


**Figure 18:** (a) CoMFA and (b) CoMSIA steric and electrostatic contour plots.

For steric interactions, the green contours indicate regions where bulky groups can increase activity, whereas yellow contours indicate regions where bulky groups can decrease activity. For electrostatic interactions, blue contours indicate regions where electropositive groups may increase activity, whereas red contours depict regions where electronegative groups may increase activity. (c) CoMSIA hydrophobic, H-bond donor and H-bond acceptor contour plots: white contours indicate regions where hydrophilic groups can increase activity, whereas yellow contours indicate regions where hydrophobic groups can increase activity, a cyan contour indicates region where H-donors may be favorable and magenta contours indicate regions where H-bond acceptor groups may be favorable to activity.

### Amides, Sulfonamides and Phthalamides

QSAR studies were also made on certain amides, sulfonamides and phthalamides (Figure 19) by few authors. For a series of thirty 4,5-dihydroxy pyrimidine carboxamide derivatives, de Melo & Ferreira [56] performed a multivariate QSAR study to obtain the correlation as:

$$\log (1/IC_{50}) = 28.67 + 127.17E_{\text{HOMO}} + 0.06\alpha_{yy} - 0.001E_T + 0.10S_{cc}$$

$$n = 30, r^2 = 0.68, r^2_{cv} = 0.53, s = 0.57, F = 28.97 \quad (3)$$

In this equation,  $E_{\text{HOMO}}$  is energy of the highest occupied molecular orbital that refers to the ionization potential

of the molecule,  $\alpha_{yy}$  refers to the component to the overall polarizability in the Y-plane,  $E_T$  stands for the total energy of the molecule and  $S_{cc}$  refers to the sum of bond electrotopological values of carbon-carbon aromatic bonds in which the carbons are not substituted. All these parameters are electronic parameters. Though the correlation with the value of  $r^2$  equal to only 0.68 is not very significant, it does describe that the ability of the molecule to be easily polarized and to donate the electron would favor the activity. These abilities of the molecule refer to their ability to easily interact with the metal ions  $Mg^{2+}$  or  $Mn^{2+}$  of the enzyme. This supports the idea that molecules may have electronic interactions with the enzyme.

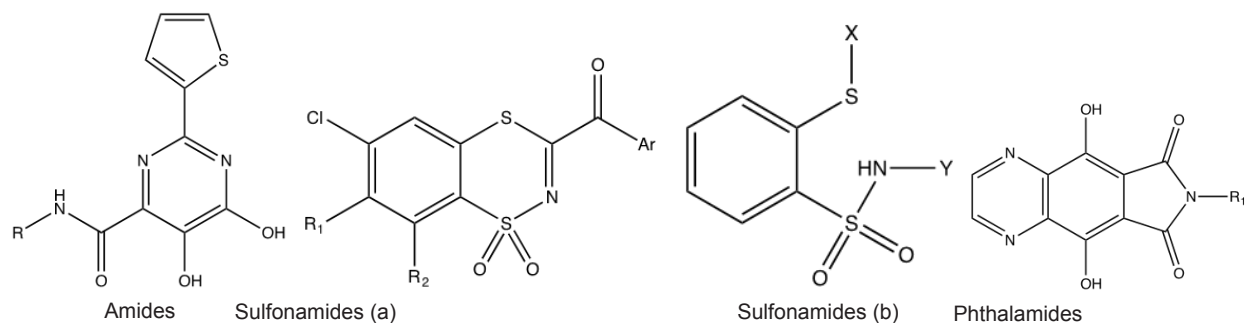


Figure 19: General structures of amides, sulfonamides and phthalamides.

Mn<sup>2+</sup> or Mg<sup>2+</sup> as cofactor is required for HIV-1 integrase activity [57]. The activity of the enzyme is optimum in the presence of Mn<sup>2+</sup>, but Mg<sup>2+</sup> is abundantly present in living cells and thus it is physiologically more relevant cation for integrase activity [58].

Some CoMFA, CoMSIA and docking studies were performed on a series of sulfonamides (Figure 19) by Gupta et al. [59]. The series of compounds and their integrase inhibitory data were taken from the literature [41,42]. The total set of 41 molecules was randomly divided into training set comprising of 31 molecules and a test set comprising of 10 molecules. The best CoMFA model had  $r^2 = 0.934$ ,  $r_{cv}^2 = 0.728$ ,  $r_{pred}^2 = 0.708$ , while the best CoMSIA model had  $r^2 = 0.928$ ,  $r_{cv}^2 = 0.794$ , and  $r_{pred}^2 = 0.59$ . The docking study was performed on the most active compound of the series that had the structure as shown in Figure 20, using FlexX program. The integrase active site has two cavities (3P and ST) which are located perpendicular to each other. The best possible binding pose and the most reliable conformation

of this most active molecule in active site were as shown in Figure 21. In the figure is also shown the X-ray crystal structure of 5CITEP (Figure 4c). According to Figure 21, the molecule as shown in Figure 20 is observed to have hydrogen bonding with Cys65, His67, and Asn155, along with the formation of a coordination ring around the Mg<sup>2+</sup> ion with sulfonamide moiety, thiol group and the nitrogen of pyrimidine ring. The two carbonyl moieties of Asp64 and Asp116 are also shown to bind with the Mg<sup>2+</sup> ion. Most of the training and test sets compounds were found to occupy the same space near the Mg<sup>2+</sup> in the vicinity of active site of HIV-1 integrase and have a common binding mode with Cys65, Asn155, and Mg<sup>2+</sup>. Thus these three interactions were found to be important to binding of these inhibitors to the enzyme. A 2D representation of interaction of the representative compound (Figure 20) is shown in Figure 22. The binding of this compound was found to be quite different from that of 5CITEP, which can be attributed to their structural diversity.

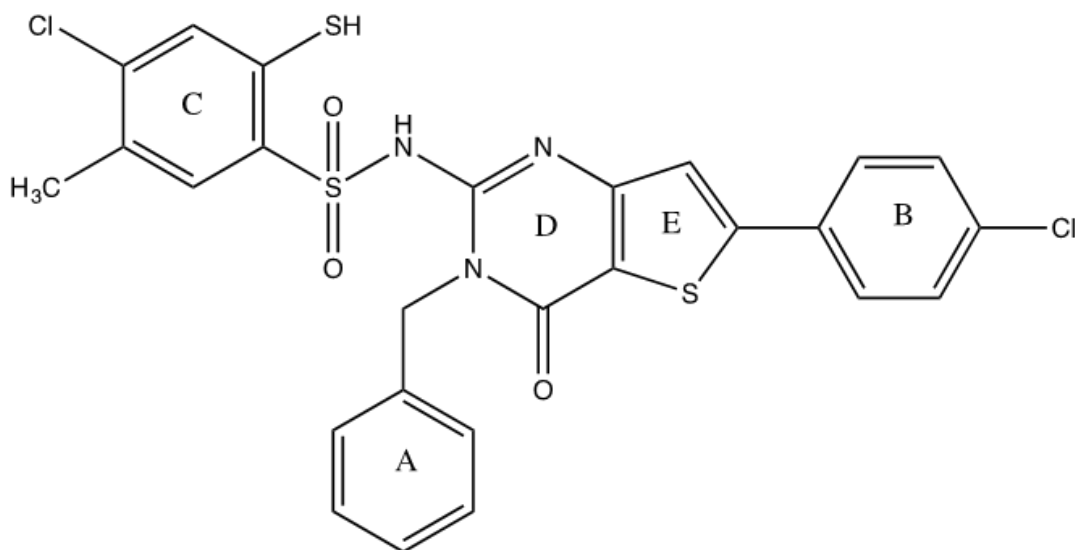
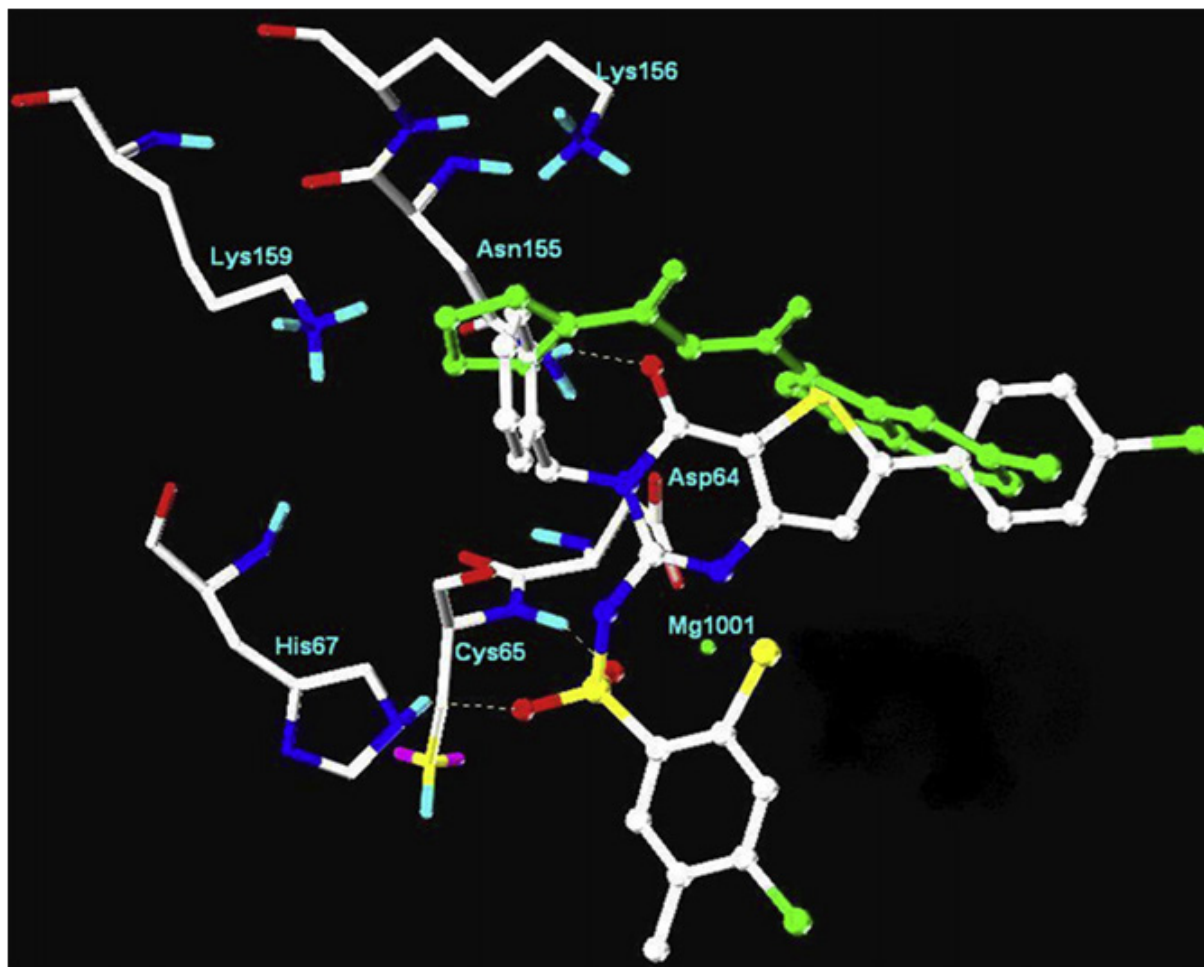
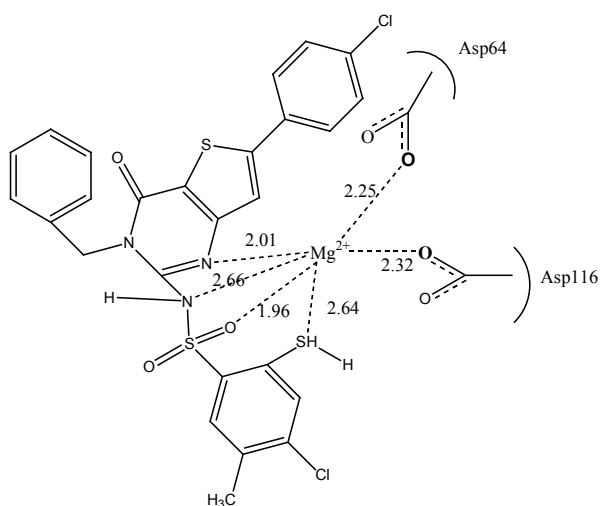


Figure 20: The structure of the most active compound of the sulfonamide series on which the docking study was performed.



**Figure 21:** A FlexX docked structure of highly active molecule (Figure 20) showing its binding in the active site of HIV-1 integrase where green ball represents coordinated  $Mg^{2+}$  ion and green capped sticks show X-ray crystallized structure of 5-CITEP.



**Figure 22:** 2D representation of interactions between  $Mg^{2+}$  ion and the inhibitor (Figure 20) obtained from docking to HIV-IN active site.

From CoMFA and CoMSIA studies favorable steric, electrostatic, and hydrophobic regions were predicted. From the CoMFA Steric contour maps (Figure 23a) drawn for the reference compound (Figure 20) for 3'-processing inhibitory activity, it was suggested that large substitutions in the region of yellow contour covering the ring E might reduce the activity. Similarly, three small yellow contours covering the phenyl ring A also suggested the regions where bulky groups would not be favored. However, large green contour covering the phenyl ring B suggested the area where a lipophilic group might be favorable as it is

surrounded by the residues Gln62, Leu63, Ile 141, Pro 142 and Thr 115 that form a lipophilic bonding pocket.

In the case of electrostatic contours (Figure 23b), red color indicated the regions where electronegative substituents might be favorable and the blue color indicated the regions where electropositive substituents might be favorable. A red contour near the sulfonamide moiety and surrounded by Cys65 and His67 indicated the region where negative or H-bond acceptor substituents might increase the activity, as these residues are H-bond donors.

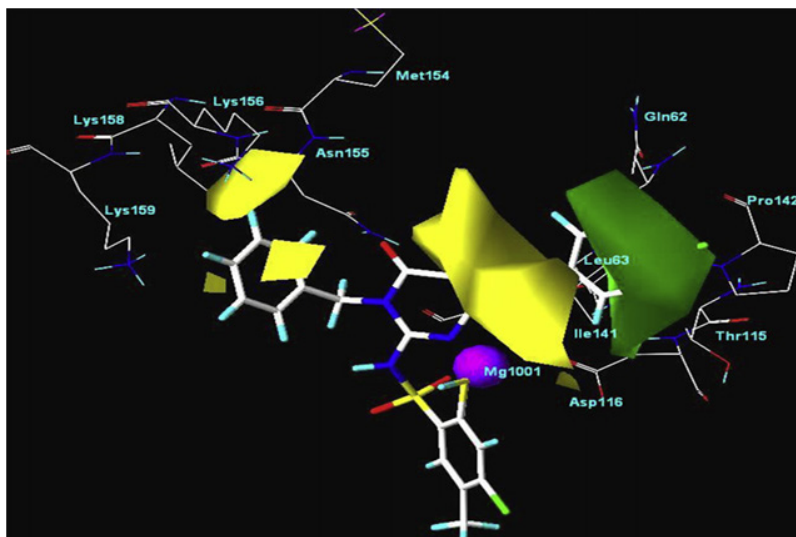


**Figure 23a:** CoMFA steric contour maps drawn with reference to compound of Figure 20.

A green contour represents sterically favored region and yellow contours represent sterically disfavored regions.

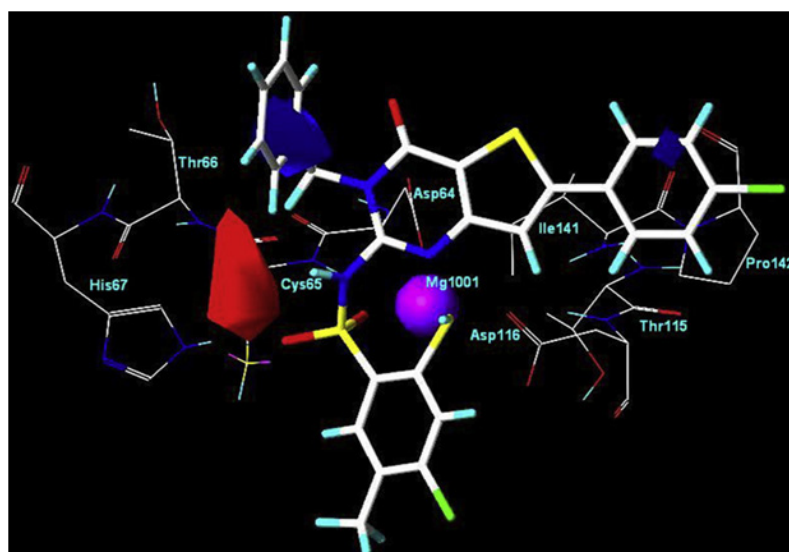


**Figure 23b:** CoMFA electrostatic contour maps for compound of Figure 20.

A red Contour represents region favorable to negatively charged substituent and blue contours the regions favorable to positively charged substituent.

In CoMSIA contour map (Figure 24) that was drawn for hydrophobic interactions, all yellow contours referred to areas where hydrophobic substituents would favor the

activity and all white contours to areas where hydrophilic substituents would favor the activity.

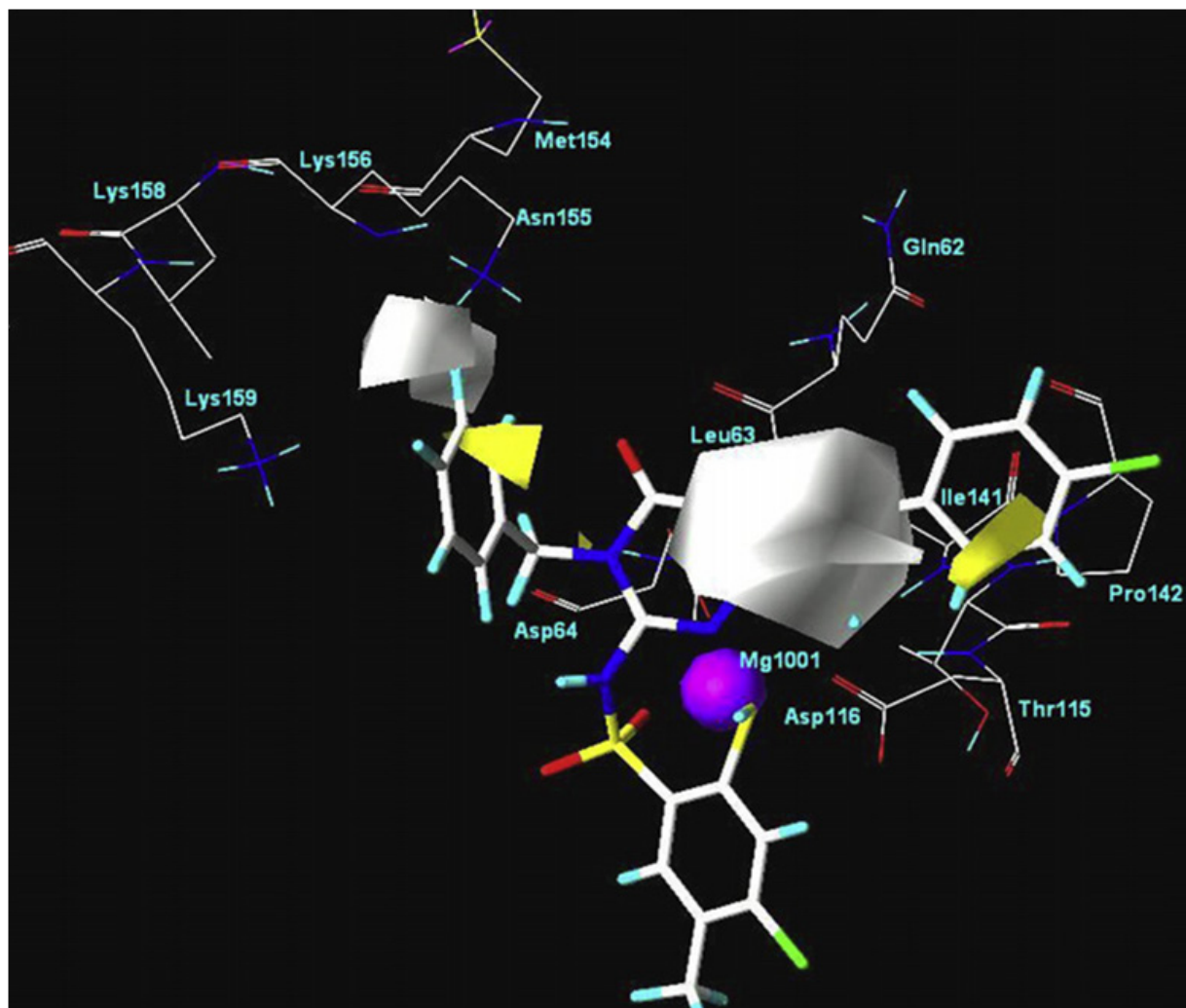


**Figure 24:** CoMSIA hydrophobic contour maps with reference to compound of Figure 20.

Yellow contours represent areas where hydrophobic substituent can be favored and white contours represent the areas where hydrophobic substituent would be disfavored.

For the series of sulfonamides (Figure 19, sulfonamides b), Kaushik et al. [60] had performed the QSAR analysis to correlate their 3'-processing and strand transfer inhibition activities as shown by eqs. 4 and 5, respectively.

### 3'-processing

$$\log(1/IC_{50}) = 0.356(\pm 0.142)\text{ClogP} + 0.050(\pm 0.032)\text{st} - 0.536(\pm 2.532)$$

$$n = 10, r = 0.913, r_{cv}^2 = 0.67, s = 0.17, F_{2,7} = 17.45 \quad (4)$$

### Strand transfer

$$\text{Log}(1/IC_{50}) = 0.27(\pm 0.089)\text{ClogP} + 0.543(\pm 0.202)\text{I} + 3.331(\pm 0.0471)$$

$$n = 15, r = 0.929, r_{cv}^2 = 0.67, s = 0.18, F_{2,12} = 37.71 \quad (5)$$

In both the equations, ClogP stands for the calculated hydrophobicity of the molecule and in eq. 4 'st' stands for surface tension and in eq. 5 'I' is an indicator parameter used for an X-substituent, being a phenyl group in sulfonamides. Its value was equal to 1 if X = a phenyl group and zero if X = H. For both 3'-processing and strand transfer, the hydrophobic property of molecules was shown to be crucial, suggesting that there could be hydrophobic interaction between the inhibitors and the enzyme. For 3'-processing, however, surface tension of the molecule was found to be important suggesting that compounds may be prone to act with the receptor in order to release its surface tension. The

negative coefficient of 'l' in eq. 5 suggested that a phenyl group attached to sulfur atom might create a steric problem.

Certain phthalimides (Figure 19) were studied for HIV-1 integrase inhibitory activity by Verschueren et al. [47]. On these compounds a Hologram QSAR (HQSAR) was performed by Magalhães et al. [61]. HQSAR introduced by Tripos Inc is a QSAR method that does not require 3D structure, putative binding conformation, and molecular alignment of the molecule, rather each molecule in the data set is divided into structural fragments that are counted in the bins of a fixed length array to form a molecular hologram. Magalhães et al. generated the molecular fragment using the following fragment distinction parameters: atoms, bonds, connections, hydrogen atoms, chirality and H-bond donor and acceptor atoms. The HQSAR model had  $r^2 = 0.972$  and  $r^2_{cv} = 0.802$ , and its contribution map had identified that the carbonyl-hydroxyl- aromatic nitrogen motif makes a positive contribution to the activity of the compounds.

Magalhães et al. [61] had also performed CoMFA studies on

these compounds to suggest that bulky groups in meta and para positions of the phenyl ring (in  $R_1$ -substituents) would increase the biological activity of this class of compounds.

### Carboxylic acid derivatives

Some quionoline carboxylic acid derivatives as shown in Figure 25 were also studied for their integrase inhibitory activity [43]. On these quionolone carboxylic acid derivatives, some CoMFA and CoMSIA studies were performed by Lu et al. [62]. Their CoMFA contour map (Figure 26) represented 80% sterically favorable and 20% sterically unfavorable area by green and yellow regions, respectively, with reference to the compound having X = o-F, m-Cl; Y = o-Me; Z = (S)-iPr. The green contours near para position of the phenyl ring and around the nitrogen of hydroquinoline ring indicated that bulky groups in these regions may be favorable to the activity. Similarly, two yellow contours, one between the hydroxyl and isopropyl groups of compound and one near the hydroquinoline ring suggested that bulky groups in these regions will decrease the activity.

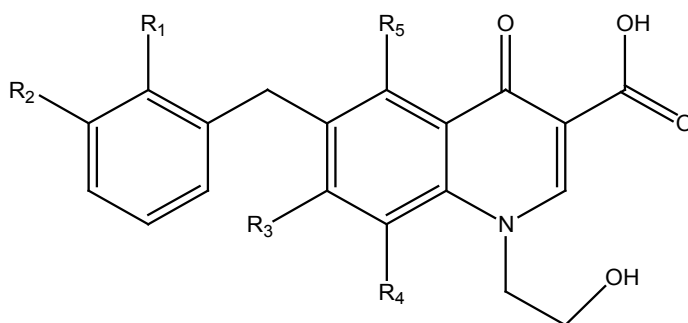


**Figure 25:** Quionoline carboxylic acid derivatives.

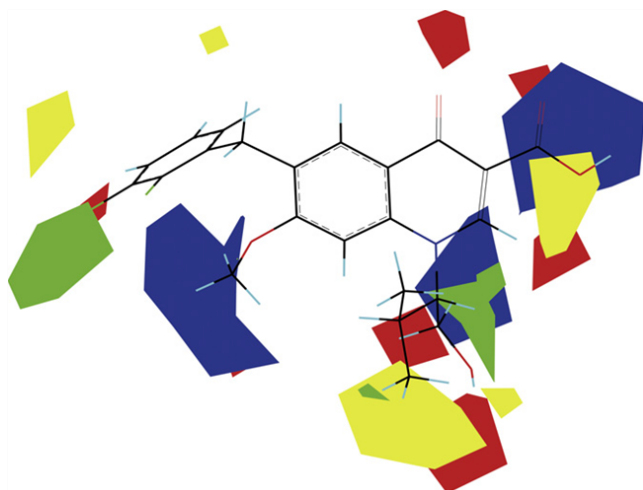


**Figure 26:** CoMFA STDEV\* coeff contour maps based on compound where X = o-F, m-Cl; Y = o-Me; Z = (S)-iPr (Figure 25).

Green contours indicate regions where steric interaction would be favored. Yellow contours are areas where the steric interaction would be disfavored. The blue region represents the area where an electro- positive group may be favorable and the red region refers to the area where an electro-negative group may be favorable.

Similarly, Figure 26 also represented electrostatically favored regions. The blue contours exhibited the favorable regions for electropositive groups (80%) and the red contours the favorable regions for electronegative groups (20%). The two large blue regions under the phenyl ring and the one near the carboxyl group are the regions where the electropositive substituents can increase the activity. Additionally, a medium blue contour distributed behind the hydroxyl group also suggested a favorable region for electropositive group. However, a red polyhedron near the ketone group of hydroquinoline ring and three red contours near the hydroxyl groups, carboxyl group, and chlorine indicated that electronegative groups around these regions might increase the inhibitory activity.

In CoMSIA contour maps (Figure 27A), the steric and

electrostatic fields were almost similar to those of CoMFA. However, the hydrophobic contour map of CoMSIA (Figure 27B) suggested that the yellow region around the para position of the phenyl ring would be favorable for the hydrophobic group, but that the four black regions near ortho position of the phenyl ring, methyl group, N-position, and carboxyl group would be unfavorable to hydrophobic group but favorable to hydrophilic substituents.

Figure 27C represented the H-bond acceptor regions. A large magenta polyhedron around the hydroquinoline ring suggested that the presence of H-bond acceptor groups in this region would increase the activity. Also a medium size magenta polyhedron in the vicinity of methoxy group might also be the region where H-bond acceptor group might increase the HIV-1 integrase inhibitory activity.

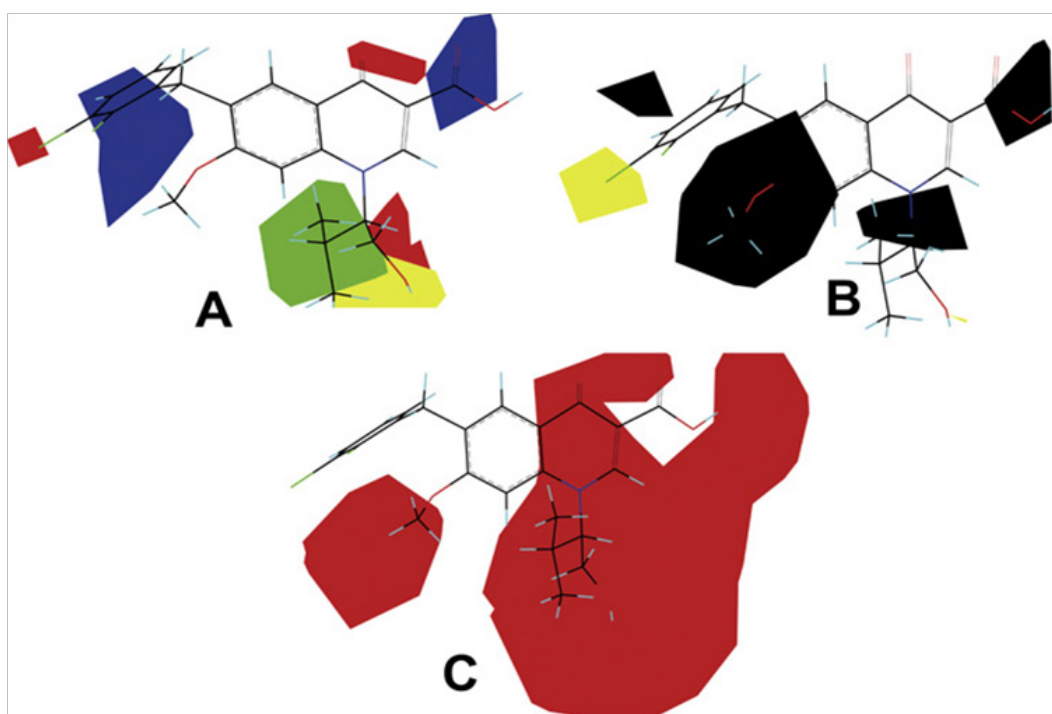


**Figure 27:** CoMSIA STDEV\*coeff contour maps based on compound where X = o-F, m-Cl; Y = o-Me; Z = (S)-iPr (Figure 25). (A) Steric and electrostatic fields: green and yellow contours represent steric favorable and unfavorable regions, respectively. Blue and red contours represent regions that favor electropositive and electronegative groups, respectively. (B) Hydrophobic fields: yellow fields indicate regions where hydrophobic groups could enhance the activity; while black fields indicate regions where hydrophobic groups decrease activity. (C) Hydrogen-bond acceptor fields: magenta and red contours represent favorable and unfavorable hydrogen-bond acceptor regions, respectively.

For the same series of quinolone carboxylic acids (Figure 25), Cheng et al. [63] performed QSAR analysis using 3D-MORSE (3D-Molecular Representation of the Structure-based Electron Diffraction) descriptors to conclude that polarizability and mass of the molecule were the most important factors governing the HIV-1 integrase inhibition activity of the molecules.

For a set of N-methyl pyrimidones (Figure 28) studied by Gardelli et al. [64] for intergrase inhibition, Kaushik et al.

[65] performed a multiple linear regression analysis and obtained a correlation as

$$\log(1/IC_{50}) = 0.773(\pm 0.24)st + 0.866(\pm 0.296)MV + 1.048(\pm 0.340)I_1 + 0.449(0.216)I_2 + 0.297(\pm 0.281)I_3 + 0.290(\pm 1.739)$$

$$n = 37, r = 0.843, r_{cv}^2 = 0.63, r_{pred}^2 = 0.71, s = 0.24, F_{5,31} = 15.22$$

(6)

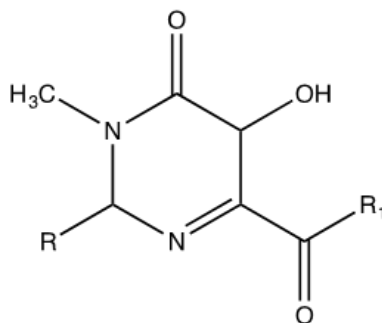


Figure 28: General structures of N-methyl pyrimidones.

In this equation  $st$  refers to the surface tension of the molecule and  $MV$  to its molar volume.  $I_1$ ,  $I_2$ , and  $I_3$  are three indicator parameters that were used, with a value of 1 each, to describe the effects of some specific structural features in the molecules.  $I_1$  was used for the presence of fluorine in R-substituent,  $I_2$  for an R-substituent being a morpholine group, and  $I_3$  for an  $R_1$ -substituent that had its phenyl moiety substituted with a fluorine atom at the para position. The positive coefficients of all these three indicator variables,

thus, indicated that the presence of fluorine and morpholine groups in the molecule will be advantageous to the activity. All these groups might be involved in some electronic interactions with the receptor. The positive coefficient of  $MV$  also suggested the involvement of the molecule in dispersion interaction with the receptor. The positive coefficient of  $st$ , however, indicated that a high value of  $st$  will make the molecule to be more prone to interact with the receptor in order to reduce its surface tension.

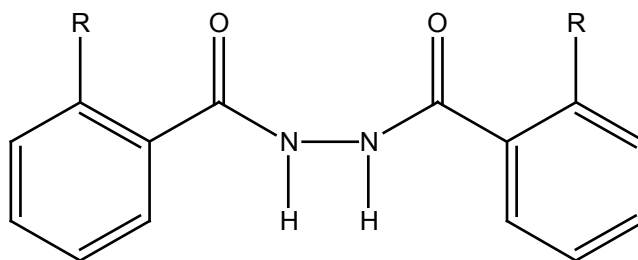


Figure 29: Structure of hydrazides.

### Hydrazides

Neamati et al. [66] made a study on a series of hydrazides, that were the analogues of *N,N'*-bis (salicylhydrazine) (Figure 29), to find out the important structural features in the compounds leading to better interaction with the integrase. A compound with  $R = OH$  was found to be a potent HIV-1 integrase inhibitor with  $IC_{50}$  value of  $2.1 (\pm 0.8) \mu M$  for 3'-processing inhibition and  $0.7 (\pm 0.1) \mu M$  for strand transfer inhibition [37]. It was shown to effectively chelate divalent cations as represented in Figure 30. When analogues of this compound were studied, most of them were found to have inhibitory concentration ( $IC_{50}$ ) less than  $3 \mu M$ , but it was noted that the presence of an OH group in all of them was essential [66].

However, it was observed by Neamati et al. [66] that several asymmetric structures exhibited similar potency as the symmetric lead inhibitor ( $R=OH$ , Figure 29). From the superimposition of the lowest-energy conformations upon

one another, these authors found, as shown in Figure 31, three important sites for ligand binding: Site A, composed of the 2-hydroxyphenyl, the R-keto, and the hydrazine moieties in a planar conformation; Site B, a hydrophobic site; and Site C, a fingerprint for the complementarity of molecular shape between ligand and the enzyme. Site A was supposed to chelate with  $Mn^{2+}$  ion in the catalytic site of the enzyme and sites B and C were assumed to be responsible for complementarity of molecular shape between ligand and receptor. Thus, only those compounds which possessed sites A, B, and C in a linear orientation were suggested to be potent inhibitors of HIV-1 integrase.

### Curcumins

Curcumins have been found to possess a variety of biological activities, such as antioxidant, anti-inflammatory, and gastrointestinal [67,68]. They also have inhibitory activity against a variety of protein kinases and phosphoryl kinase [69], and can inhibit carcinogenesis and cancer

growth [70,71]. More recently, curcumin has been reported to inhibit HIV replication [72] by inhibiting particularly HIV-1 integrase. It inhibits both the strand transfer and 3'-processing activities with  $IC_{50}$  of 40 and 30  $\mu$ M, respectively [73-75]. Curcumin and related compounds have also been found to inhibit HIV-1 and HIV-2 proteases with  $IC_{50}$  of 100 and 250  $\mu$ M, respectively [76]. Vajragupta et al. [77] studied the mode of interaction of curcumin with HIV-1 integrase. According to these authors, the binding site of IN is formed by residues Asp64, His67, Thr66, Glu92, Thr93, Asp116, Ser119, Asn120, and Lys159. When these authors docked the curcumin in the core domain, they found that curcumin contacts the catalytic residues adjacent to Asp116 and Asp64, and near the divalent metal ion,  $Mg^{2+}$ . For docking, the crystal structure 1QS4.pdb of the core domain of HIV-1

IN (residues C56–Q209) complexed with inhibitor 5CITEP was used to prepare IN active binding site. Figures 32 & 33 show the binding mode of curcumin with the IN. Figure 33 shows that ket-enol oxygens of curcumin are located adjacent to the catalytic residues Asp116, Asp64, and Glu92 of the enzyme and are within the coordination range of  $Mg^{2+}$ . One of the terminal phenol moieties forms H-bonds with His67, Thr66, and Lys155 inside a cavity with a large surface area and the other one is within hydrogen bonding range of Asn120, Ser119, and Thr93. Further, it can be seen that the curcumin molecule involves both strand transfer and 3'-processing areas of active site, where its phenolic oxygen can interact with Lys156 to inhibit strand transfer and o-methoxy group with His67 and Thr66 to inhibit 3'-processing activity.

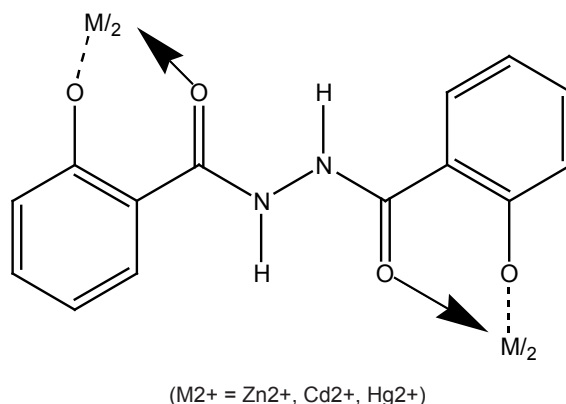


**Figure 30:** A diagrammatic representation of chelating of a compound with R=OH (Figure 29) with a divalent metal ion.

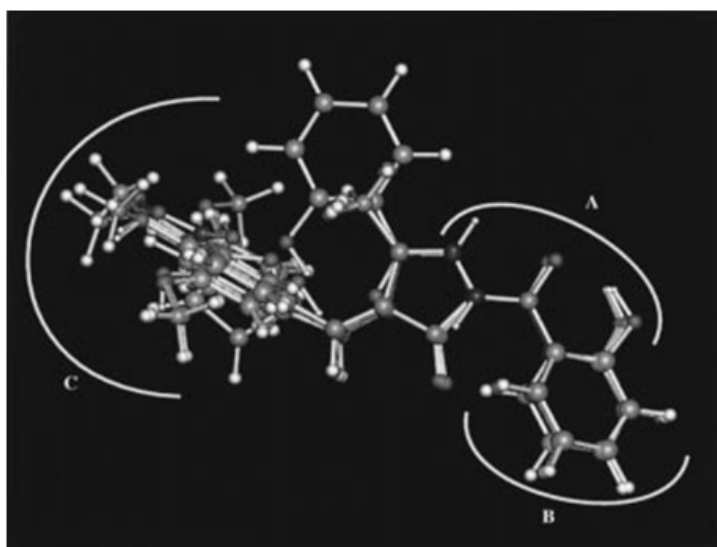


**Figure 31:** Superimposition of all the active compounds in the "ball-and-stick" model.

Site A depicts the metal chelation site or hydrogen-bonding region, site B, the hydrophobic region, and site C, a fingerprint for the complementarity of molecular shape between ligand and enzyme.

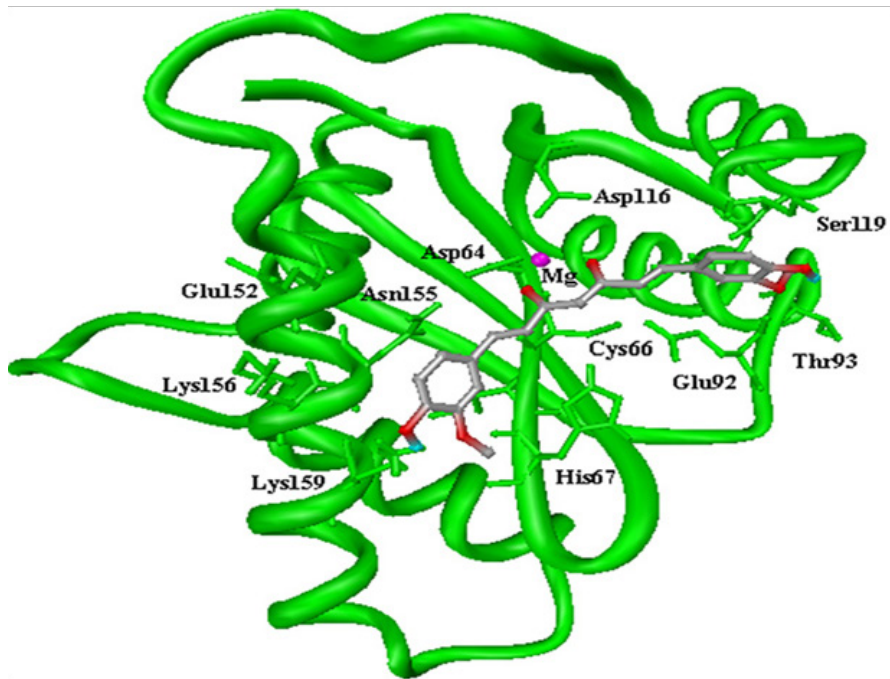


**Figure 32:** The bound conformation of curcumin in the active site of HIV-1 IN, where the backbone of catalytic site of enzyme is shown by green, in which interacting amino acid residues by sticks. The curcumin molecule is shown with ash color. A Mg<sup>2+</sup> ion is shown by a ball in magenta color.

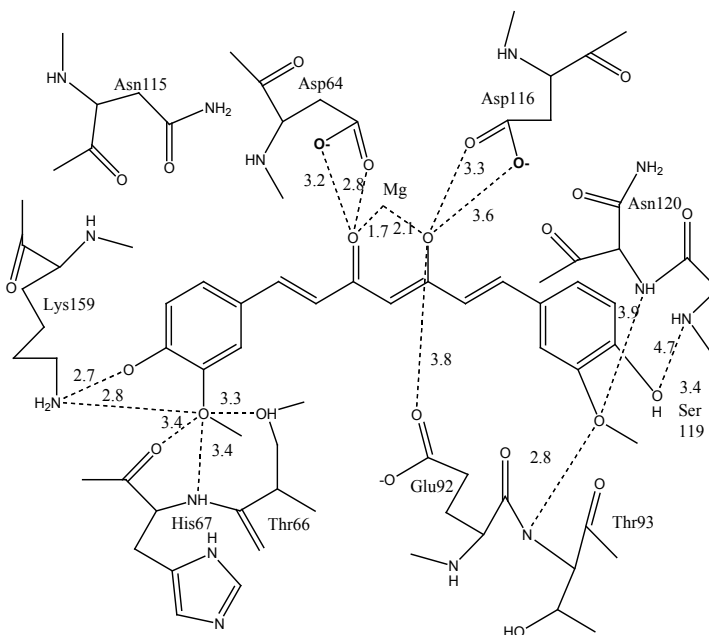


**Figure 33:** A schematic diagram showing interactions of curcumin with HIV-1 integrase.

### β-Diketoacids (BDKAs)

For a fruitful structure-based drug design, there should be a well defined X-ray crystal structure of the enzyme. Notwithstanding, there are 15 crystal structures of HIV-1 IN

currently available and remarkable differences are observed in the conformation of the active site in all these reported X-ray structures. Thus, the lack of a well-defined crystal structure of IN and also simultaneously the lack of a *bona*

*vide* lead molecule greatly hampered the design of potent IN inhibitors. But the recent discovery of  $\beta$ -diketoacids as IN inhibitors provided a lead molecule [78] that led to discover the first molecule S1360 (Figure 34) to enter the clinical trials against HIV-1 infection. This molecule is actually a bioisostere of  $\beta$ -diketoacid and is orally active against HIV-1 [79]. The other two important compounds were BDKA (bis-diketoacid) and 5CITEP (1-(5-chloroindol-3-yl)-3-

hydroxy-3-(2H-tetrazo-5-yl)-propenone). 5CITEP is also a bioisostere of  $\beta$ -diketoacid, possessing a 5-chloro-indole moiety. Both S1360 and 5CITEP are selective inhibitors of strand transfer reaction. BDKA has two  $\beta$ -diketoacid functional groups on 1,3-positions of the central phenyl ring. It inhibits both the 3'-processing and strand transfer reactions of IN with comparable  $IC_{50}$  values [80,81].

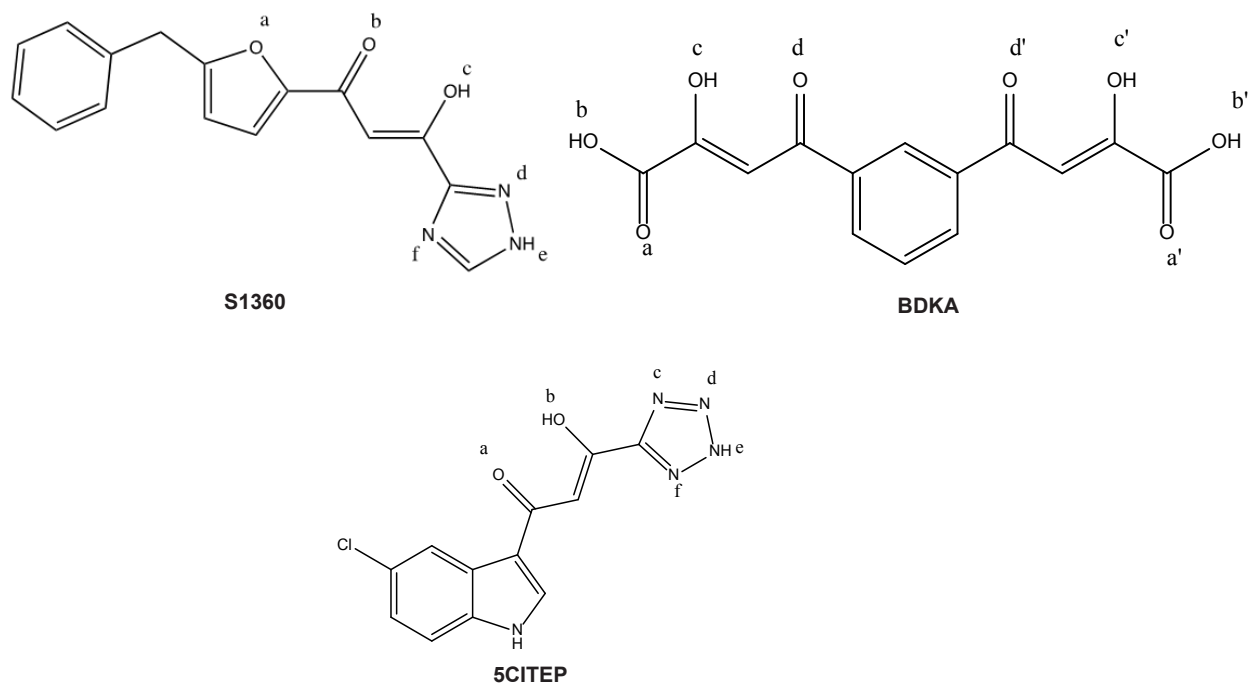


**Figure 34:** Some important  $\beta$ -diketoacid analogues studied for HIV-1 IN inhibitions. BDKA: bis-diketoacid, 5CITEP:1-(5-chloroindol-3-yl)-3-hydroxy-3-(2H-tetrazo-5-yl)-propenone

Dayam & Neamati [82] performed docking studies on these three compounds as shown in Figure 34 in order to predict their biologically relevant conformations when bound to IN active site. Of the several core domain structures available for IN, only two were found to have completely resolved active sites (chain B in PDB 1BIS and chain C in PDB 1BL3) [83,84]. Remarkable differences were observed in the conformations of these two substrate free active sites. An X-ray structure of the core domain of IN in complex with 5CITEP was reported (PDB 1QS4) [33]. The conformation of the flexible loop as well as the entire active site in the IN–5CITEP complex was found to largely differ from the above two structures. The active site regions from these three structures were designated as active site A (from chain A in PDB 1QS4), active site B (from chain B in PDB 1BIS), and active site C (from chain C in PDB 1BL3), all of which were found to be complexed with  $Mg^{2+}$  ion (Figure 35). The carbonyl oxygen atoms of two residues of DDE motif, D64 and D116, occupy two of the six coordination positions of the  $Mg^{2+}$  ion. The DDE motif, a triad of acidic residues D64, D116, and E152, involves in the binding of metal cofactor

and potentially induces certain conformational changes in the catalytically active region of IN, which in turn makes IN ready for its catalytic process [85,86].

When Dayam & Neamati [82] made docking studies on  $\beta$ -diketoacid analogues as given in Figure 34, they found that the conformational flexibility of the flexible loop does not strongly influence BKDA and it adopts fairly similar bound conformation in all three active sites A, B, and C and establishes strong interaction with catalytically important residues in both ST and 3P cavities, inhibiting both stand transfer and 3'-processing reactions with comparable potency. Thus it could be concluded that the inhibitor that could form strong interactions with amino acid residues in both ST and 3P cavities of the IN active site would inhibit both stand transfer and 3'-processing reactions with similar potency. S1360 was found to adopt similar bound conformation only in active sites A and C, but quite different in active site B. Several studies have indicated that the conformation of the active site B is biologically relevant active site conformation of IN in which the flexible loop

adopts an extended conformation. Interestingly, none of bound conformations of 5CITEP studied by Dayam and Neamati, using the GOLD docking package, precisely resembled that of bound conformation in the reported crystal structure of the IN-5CITEP complex. However, the bound location of the 5CITEP in active site B was found close to the bound location of 5CITEP in the crystal structure.

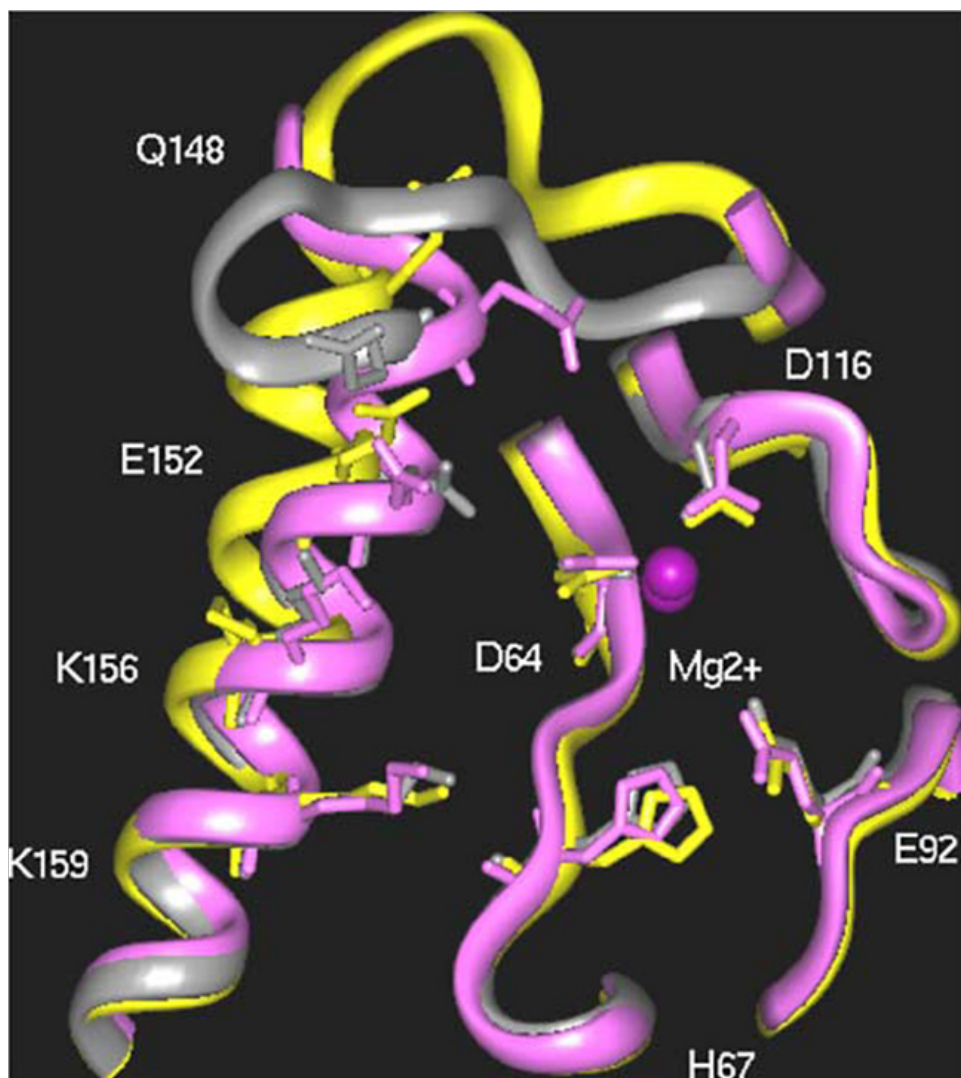


**Figure 35:** The superimposed backbone ribbon models of the active site regions from three different crystal structures.

The pink (PDB 1QS4), yellow (PDB 1BIS), and gray (PDB 1BL3) ribbons represent the active site A, B, and C, respectively. The  $Mg^{2+}$  ions are shown in magenta.

### Structurally different classes of compounds

Several authors performed QSAR studies on a few series of HIV-1 integrase inhibitors comprised of structurally different classes of compounds in order to find common modalities of drug-receptor interactions for integrase inhibition. Yuan & Parrill [87] took a set of 11 different structural classes that included tyrophostins, coumarins, aromatic sulfonamides,

chioric acids, tetracyclines and so on and performed a QSAR study on them using genetic function approximation. The best QSAR model derived for the complete set of 11 classes indicated that the compounds may differ in exact relationship between structure and inhibition, perhaps through interactions with different subsets of amino acids in the binding pocket of the enzyme or through the presence of non-overlapping binding pockets. However,



when 11 different classes were divided into two clusters, one consisting of five structural features and the other six, and two different models were obtained, it was found that the compounds of larger clusters might bind near the metal ion in a fashion similar to that observed in one publically available co-crystal structure of an inhibitor bound to HIV-1 integrase. Flexible alignment of inhibitors in two clusters led to define two different pharmacophores consistent with previously published pharmacophores [88,89]. In a later study also, Yuan & Parrill [90] showed that these two clusters of compounds might have two separate binding sites.

Makhija & Kulkarni [91] performed a CoMSIA study on a set

of integrase inhibitors consisted of five structurally diverse classes: salicylpyrazolinones, dioxepinones, coumarins, quinones and benzoic hydrazides. These compounds were evaluated for both 3'-processing and strand transfer inhibition activities. The CoMSIA model obtained for 3'-processing had  $r^2_{cv} = 0.821$ ,  $r^2_{pred} = 0.608$  and for strand transfer  $r^2_{cv} = 0.759$ ,  $r^2_{pred} = 0.660$ , and its contours maps obtained for the compound, a salicylpyrazolinone (Figure 36), as template, had indicated that the steric bulk in the vicinity of the two phenyl rings would be favorable for both 3'-processing and 3'-strand transfer inhibition activities and that the hydroxyl group and the carbonyl functions of the pyrazole ring would be involved in electrostatic interaction in both the activities.

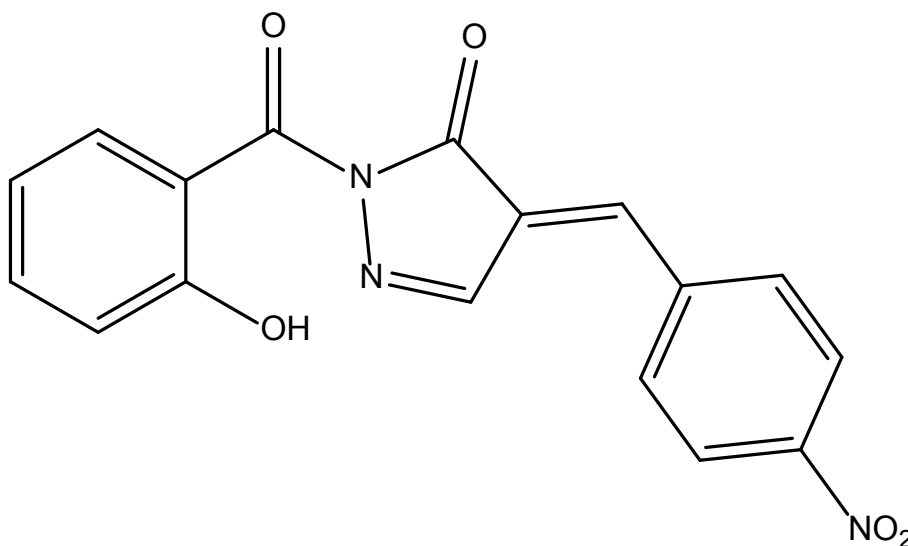


**Figure 36:** Structure of a salicylpyrazolinone.

The hydrophobic contour maps of CoMSIA had exhibited that for 3'-processing the hydrophobically disfavored region surrounded almost the entire molecule, whereas for strand transfer activity the hydrophobically disfavored regions surrounded the terminal phenyl ring and some parts of the pyrazolinone nucleus. The H-bond donor and acceptor contour maps indicated that salicylic hydroxyl group might act as H-bond donor and the hydrazide function and  $\text{NO}_2$  group as H-bond acceptors in both the activities.

A set of 213 compounds across 12 structurally diverse classes of HIV-1 integrase inhibitors was subjected to QSAR study by Iyer & Hopfinger [92] in which they used 4D fingerprints and classic QSAR descriptors. The 12 structurally diverse classes were partitioned into five clusters and then for each one of them a QSAR model, overwhelmingly composed of 4D fingerprint descriptors, was obtained. Analysis of these models suggested that compounds of three clusters might bind at a common site on the enzyme through a common H-bond donor at the inhibitors, but involving somewhat

different alignment and/or poses for the inhibitors of each of the three different clusters. The particular alignment of compounds in these clusters depended on their nonpolar groups. The QSAR models derived for other two clusters, one for coumarins and other for depsides and depsidones, were based on less defined pharmacophores.

For almost the same set of compounds of structurally different classes as treated by Iyer and Hopfinger, Nunthaboot et al. [93] performed CoMFA and CoMSIA studies. The biological data for 3'-processing inhibition were used. The CoMFA model obtained had  $r^2 = 0.957$ ,  $r^2_{cv} = 0.678$ , and  $r^2_{pred} = 0.719$  and CoMSIA model had  $r^2 = 0.872$ ,  $r^2_{cv} = 0.693$  and  $r^2_{pred} = 0.568$ . The CoMFA and CoMSIA contour maps obtained by these authors as shown by Figures 37-39, respectively, suggested the regions favorable to bulky groups, positively or negatively charged substituents, and H-bond donor or acceptor moieties. The CoMFA contour map (Figure 37a) suggested that bulky groups might be favorable to the activity in a plane of indole ring (large green contour). The sterically

preferred region was found to be located near hydrophobic amino acid residues Phe121 and Phe139 of the enzyme. With the side chains of these residues, the bulky aromatic substituents might have hydrophobic interactions. Another sterically favorable region was suggested to be close to chloroindole ring of 5CITEP. Three yellow contours located around the tetrazole ring suggested the areas where small bulky groups might be favorable to the activity.

In CoMFA electrostatic contour plots (Figure 37b), the positively charged favored regions (blue) were observed to be near Glu148 and Glu149 residues of the enzyme,

where electron-deficient groups might interact with side chains of these residues. Another favorable region for electron deficient substituents was near the nitrogen atom of the indole ring of 5CITEP. Red contours exhibiting the favorable regions for negatively charged substituents were shown near the CH adjacent to the carbonyl and hydroxyl carbons of 5CITEP. The red contours are in fact close to  $Mg^{2+}$  located between Asp64 and Asp 116 residues of integrase. The aromatic moiety common to many integrase inhibitors have been proposed to interact with this divalent cation with a cation- $\pi$  type of interaction [66,94].

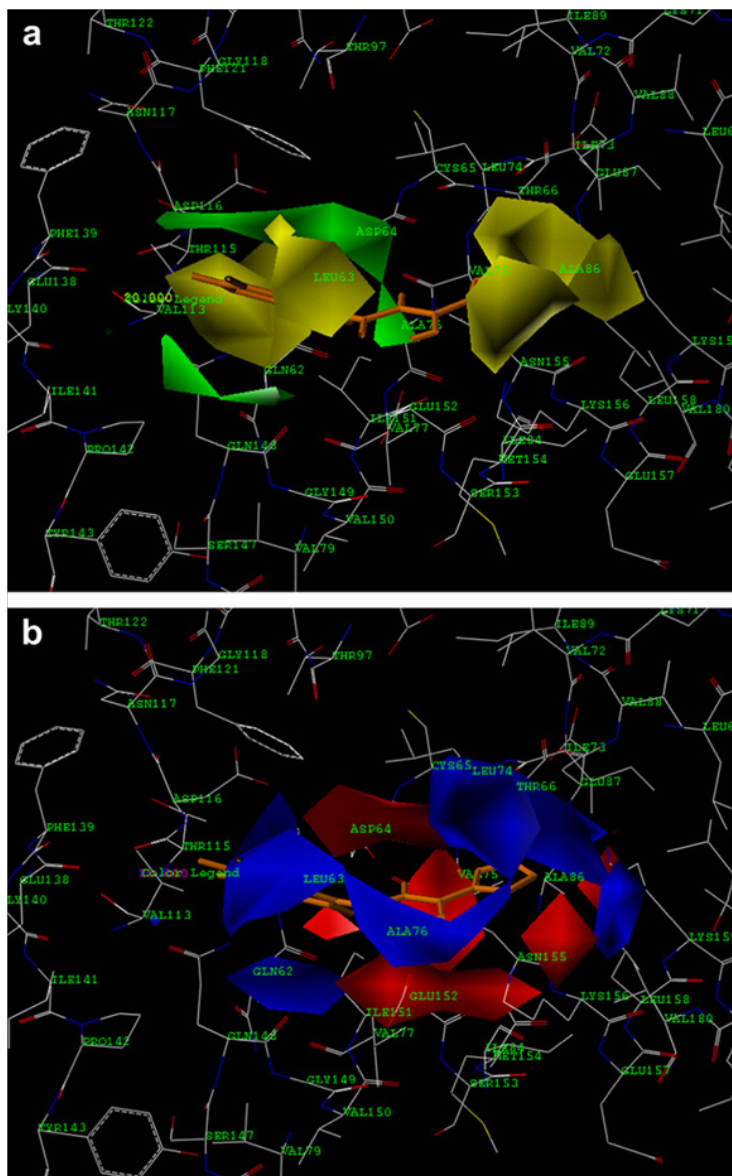


**Figure 37:** CoMFA contour maps: (a) steric fields; green contours represent sterically favored regions, yellow contours indicate sterically disfavored regions, (b) electrostatic fields; red contours represent negative potential favored regions and blue regions indicate positive charge favored regions. The contours were mapped into the active site of HIV-1 IN and 5CITEP was displayed for reference.

The CoMSIA contour maps for H-bond donors (Figure 38) indicated through cyan color the two favorable regions for H-bond donors. The first one was near the CH adjacent to carbonyl carbon and to the hydroxyl carbon of 5CITEP and the second was near the indole ring of 5CITEP. Four purple contours around the tetrazole ring indicated that H-bond donor groups in this area might decrease the activity. The CoMSIA H-bond acceptors fields were shown in Figure 39, where a magenta contour near the keto-enol moiety of

5CITEP suggested a favorable region for H-bond acceptor group. This favorable region near the keto-enol moiety for H-bond acceptor group supported the pharmacophore model proposed by Barreca et al. for diketo acid analogues [95]. A large red contour behind the NH moiety of the indole ring of 5CITEP had however, suggested, that H-bond acceptor features of ligands in this area might not be favorable to the inhibition activity.

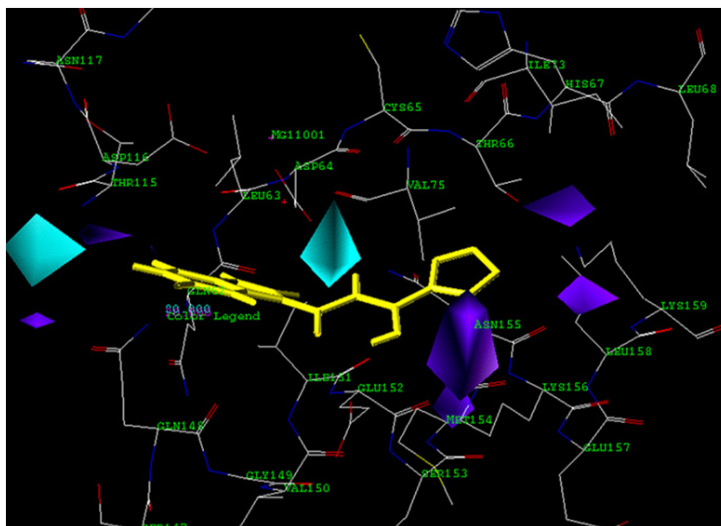


**Figure 38:** CoMSIA hydrogen bond donor contour plots within the active site of the complex structure of HIV-1 IN/5CITEP. Cyan contours represent areas where hydrogen-bond donor groups on ligand enhance activity, whereas purple contours indicate areas where hydrogen-bond donor groups on ligand decrease activity.

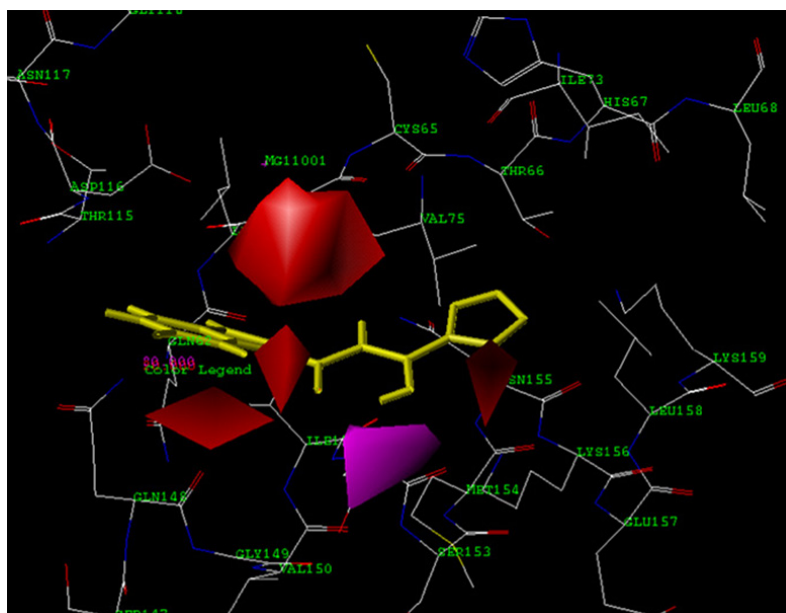


**Figure 39:** CoMSIA hydrogen bond acceptor contour plots within the active site of the complex structure of HIV-1 IN/5CITEP. Magenta contours represent regions where hydrogen-bond acceptor groups on ligand can enhance activity, while red contours indicate areas where hydrogen bond-acceptor groups on ligand can decrease activity.

## An Overall View

A large number of potent HIV-1 integrase inhibitors have been found to have, in common, two aryl units separated by a central linker, where one of these aryl moieties must contain 1, 2-dihydroxy substituents. The hydroxyl groups were found to be important for the interaction with the enzyme. The integrase active sites also have been found to accommodate large variations in ligand size and shape and different binding modes.

Most of the compounds have been found to inhibit both 3'-processing and strand transfer reactions involved in the viral integration by integrase. These two reactions represent a transesterification reaction requiring the presence of divalent cations  $Mn^{2+}$  and  $Mg^{2+}$ . For catechols, both 3'-processing and strand transfer inhibition activities were found to be controlled by some electronic descriptors, shape related physicochemical parameters, and some thermodynamic descriptors related to desolvation phenomena during binding. On the basis of some studies, a 6-point pharmacophore for IN inhibition was defined which should have two H-bond acceptor groups, two hydrophobic groups, a negative feature (N), and an aromatic ring (R).

For certain IN inhibitors, the ability of the molecule to be easily polarized and to donate the electrons were found to favor the activity, as these properties might enable them to easily interact with the metal ions  $Mg^{2+}$  or  $Mn^{2+}$  of the enzyme. Certain categories of the inhibitors were found to have hydrogen binding with the active site of the enzyme along with the formation of a coordination ring around the  $Mg^{2+}$ . Hydrophobic property, polarizability, and mass of molecules were also found to be important factors governing the integrase inhibition activity of compounds. In a recent communication, Garg & Ko [96] had also concluded that integrase inhibition did involve hydrophobic, steric, and electrostatic interactions, though in many QSAR models discussed by them hydrophobic descriptors were not found to be important. However, since there are certainly hydrophobic binding sites in integrase, it was suggested by Garg and Ko that ligands might induce some conformational changes in the binding sites, because of which they might become unable to have any hydrophobic interaction with the ligands.

For structurally different classes of compounds it was found that compounds may differ in exact relationship between structure and inhibition, perhaps through interactions with different subsets of amino acids in the binding pocket of the enzyme or through the presence of non-overlapping binding pockets. The aromatic moiety common to many integrase inhibitors have been proposed to interact with the cation  $Mg^{2+}$  involving a cation- $\pi$  type of interaction.

## References

- Isselbacher KJ, Eugene B, Wilson J, Martin JB, Fauci AS, et al. (1994) In Harrison's principles of internal medicine, McGraw Hill, New York, (b) Gallo RC (1987) The aids virus. Sci Am 256: 46-56.
- Fauci AS (1988) The human immunodeficiency virus: Infectivity and mechanisms of pathogenesis. Science 239(4840): 617-622.
- De Clercq E (1995) Toward improved anti-HIV chemotherapy: Therapeutic strategies for intervention with HIV infections. J Med Chem 38(14): 2491-2517.
- De Clercq E (1999) Perspectives of non-nucleoside reverse transcriptase inhibitors (NNRTIs) in the therapy of HIV-1 infection. IIFarmaco 54(1-2): 26-45.
- Wlodawer A, Ericson JW (1993) Structure-based inhibitors of HIV-1 protease. Annu Rev Biochem 62: 543-85.
- Babine RE, Bender SL (1997) Molecular recognition of protein-ligand complexes: Applications to drug design. Chem Rev 97(5): 1359-1472.
- Garg R, Gupta SP, Gao H, Mekapati SB, Debnath AK, et al. (1999) QSAR studies on anti HIV-1 drugs. Chem Rev 99(12): 3525-3601.
- Gupta SP (2002) Advances in QSAR studies of HIV-1 reverse transcriptase inhibitors. Prog Drug Res 58: 223-264.
- Gupta SP, Nagappa AN (2003) Design and development of integrase inhibitors as anti-HIV agents. Curr Med Chem 10(18): 1779-1794.
- Bushman FD, Craigie R (1991) Activities of human immunodeficiency virus (HIV) integration protein *in vitro*: specific cleavage and integration of HIV DNA. Proc Natl Acad Sci USA 88(4): 1339-1343.
- Engelman A, Mizuuchi K, Craigie R (1991) HIV-1 DNA integration: mechanism of viral DNA cleavage and DNA strand transfer. Cell 67(6): 1211-1221.
- Vinc C, Plasterk RHA (1993) The human immunodeficiency virus integrase protein. Genet 9(12): 433-438.
- Fesen MR, Kohn KW, Leteurtre F, Pommier Y (1993) Inhibitors of human immunodeficiency virus integrase. Proc Natl Acad Sci USA 90(6): 2399-2403.
- Snasel J, Rejman D, Liboska R, Tocik Z, Ruml T, et al. (2001) Inhibition of HIV-1 integrase by modified oligonucleotides derived from U5' LTR. Eur J Biochem 268(4): 980-986.
- Mazumder A, Raghavan K, Weinstein JN, Kohn KW, Pommier Y (1995) Inhibition of human immunodeficiency virus type-1 integrase by curcumin. Biochem Pharmacol 49(19): 1165-1170.
- Mazumder A, Neamati N, Sunder S, Schultz J, Pertz H, et al. (1997) Curcumin analogs with altered potencies against HIV-1 integrase as probes for biochemical mechanisms of drug action. J Med Chem 40(19): 3057-3063.
- Engelman A, Craigie R (1992) Identification of conserved amino acid residues critical for human immunodeficiency virus type 1 integrase function *in vitro*. J Virol 66(11): 6361-6369.
- Kulkosky J, Jones KS, Kat RA, Mack JP, Skalka AM (1992) Residues critical for retroviral integrative recombination in a region that is highly conserved among retroviral/retrotransposon integrases and bacterial insertion sequence transposases. Mol Cell Biol 12(5): 2331-2338.
- Polard P, Chandler M (1995) Bacterial transposases and retroviral integrases. Mol Microbiol 15(1): 13-23.

20. Rowland SJ, Dyke KG (1990) Tn552, a novel transposable element from *Staphylococcus aureus*. *Mol Microbiol* 4(6): 961-975.
21. Fesen MR, Pommier Y, Leteurtre F, Hiroguchi S, Yung J, et al. (1994) Inhibition of HIV-1 integrase by flavones, caffeic acid phenethyl ester (CAPE) and related compounds. *Biochem Pharmacol* 48(3): 595-608.
22. Mazumder A, Gazit A, Levitzki A, Nicklaus M, Yung J, et al. (1995) Effects of tyrphostins, protein kinase inhibitors, on human immunodeficiency virus type 1 integrase. *Biochemistry* 34(46): 15111-15122.
23. Zaho H, Neamati N, Mazumder A, Sunder S, Pommier Y, et al. (1997) Arylamide inhibitors of HIV-1 integrase. *J Med Chem* 40(8): 1186-1194.
24. Lafimina RL, Graham PL, Legrow K, Hastings JC, Wolfe A, et al. (1995) Inhibition of human immunodeficiency virus integrase by bis-catechols. *Antimicrob Agents Chemother* 39(2): 320-324.
25. Lin Z, Neamati N, Zhao H, Kiryu Y, Turpin JA, et al. (1999) Chioric acid analogues as HIV-1 integrase inhibitors. *Med Chem* 42(8): 1401-1414.
26. Molteni V, Rhodes D, Rubins K, Mansen M, Bushman FD, et al. (2000) A new class of HIV-1 integrase inhibitors: the 3,3,3', 3'-tetramethyl-1,1'-spirobi(indan)-5,5',6,6'-tetrol family. *J Med Chem* 43(10): 2031-2039.
27. Cotellet P, Cateau JP (1997) A Convenient Synthesis of Substituted 2-Phenyl-naphthalenes From Phenylacetones. *Tetrahedron Lett* 38(17): 2969-2972.
28. Dupont R, Cotellet P (1998) Reaction of aryloxyacetals with boron tribromide. *Tetrahedron Lett* 39(46): 8457-8460.
29. Dupont R, Cotellet P (1999) The reaction of arylacetones with boron tribromide. *Synthesis* 9: 1651-55.
30. Dupont R, Jeanson L, Mouscadet JF, Cotellet P (2001) Synthesis and hiv-1 integrase inhibitory activities of catechol and bis-Catechol derivatives. *Bioorg Med Chem Lett* 11(24): 3175-3178.
31. Farnet CM, Wang B, Hansen M, Lipford JR, Zalkow L, et al. (1998) Human Immunodeficiency Virus Type 1 cDNA Integration: New Aromatic Hydroxylated Inhibitors and Studies of the Inhibition Mechanism. *Antimicrob Agents Chemother* 42(9): 2245-2253.
32. Espeseth AS, Felock P, Wolfe A, Witmer M, Grobler J, et al. (2000) HIV-1 integrase inhibitors that compete with the target DNA substrate define a unique strand transfer conformation for integrase. *Proc Natl Acad Sci USA* 97(21): 11244-11249.
33. Goldgur Y, Craigie R, Cohen GH, Fujiwara T, Yoshinaga T, et al. (1996) Structure of the HIV-1 integrase catalytic domain complexed with an inhibitor: a platform for antiviral drug design. *Proc Natl Acad Sci USA* 96(23): 13040-13043.
34. King PJ, Ma G, Miao W, Jia Q, McDougall BR, et al. (1999) Structure-activity relationships: analogues of the dicaffeoylquinic and dicaffeoyltartaric acids as potent inhibitors of human immunodeficiency virus type 1 integrase and replication. *J Med Chem* 42(3): 497-509.
35. Nicklaus MC, Neamati N, Hong H, Mazumder A, Sunder S, et al. (1997) HIV-1 integrase pharmacophore: discovery of inhibitors through three-dimensional database searching. *J Med Chem* 40(6): 920-929.
36. Hong H, Neamati N, Wang S, Nicklaus MC, Mazumder A, et al. (1997) HIV-1 integrase pharmacophore: discovery of inhibitors through three-dimensional database searching. *J Med Chem* 40(6): 930-936.
37. Zaho H, Neamati N, Sunder S, Hong H, Wang S, et al. (1997) Hydrazide-containing inhibitors of HIV-1 integrase. *J Med Chem* 40(6): 937-941.
38. Neamati N, Mazumder A, Sunder S, Owen JM, Tandon M, et al. (1998) Highly potent synthetic polyamides, bisdistamycins, and lexitropsins as inhibitors of human immunodeficiency virus type 1 integrase. *Mol Pharmacol* 54(2): 280-290.
39. Neamati N, Hong H, Sunder S, Milne GWA, Pommier Y (1997) Potent inhibitors of human immunodeficiency virus type 1 integrase: identification of a novel four-point pharmacophore and tetracyclines as novel inhibitors. *Mol Pharmacol* 52(6): 1041-1055.
40. Deng J, Sanchez T, Al-Mawsawi LQ, Dayam R, Yunes RA, et al. (2007) Discovery of structurally diverse HIV-1 integrase inhibitors based on a chalcone pharmacophore. *Bioorg Med Chem* 15(14): 4985-5002.
41. Brzozowski Z, Saczewski F, Sanchez T, Kuo CL, Gdaniec M, et al. (2004) Synthesis, antiviral, and anti-HIV-1 integrase activities of 3-aryl-1,1-dioxo-1,4,2-benzodithiazines. *Bioorg Med Chem* 12(13): 3663-3672.
42. Brzowski Z, Slawinski J, Saczewski F, Sanchez T, Neamati N (2008) Synthesis, anti-HIV-1 integrase, and cytotoxic activities of 4-chloro-N-(4-oxopyrimidin-2-yl)-2-mercaptobenzenesulfonamide derivatives. *Eur J Med Chem* 43(6): 1188-1198.
43. Sato M, Kawakami H, Motomura T, Aramaki H, Matsuda T, et al. (2009) Quinolone carboxylic acids as a novel monoketo acid class of human immunodeficiency virus type 1 integrase inhibitors. *J Med Chem* 52(15): 4869-4882.
44. Cheng P, Huang N, Jiang ZY, Zhang Q, Zheng YT, et al. (2008) 1-Aryl-tetrahydroisoquinoline analogs as active anti-HIV agents *in vitro*. *Bioorg Med Chem Lett* 18(7): 2475-2478.
45. Mekour K, Mouscadet JF, Desmæle D, Subra F, Leh H, et al. (1998) Styrylquinoline derivatives: a new class of potent HIV-1 integrase inhibitors that block HIV-1 replication in CEM cells. *J Med Chem* 41(15): 2846-2857.
46. Zouhiri, F, Mouscadet JF, Mekouar K, Desmæle D, Savoure D, et al. (2000) Structure-activity relationships and binding mode of styrylquinolines as potent inhibitors of HIV-1 integrase and replication of HIV-1 in cell culture. *J Med Chem* 43(8): 1533-1540.
47. Verschueren WG, Dierynck I, Amssoms KI (2005) Design and optimization of tricyclic phtalimide analogues as novel inhibitors of HIV-1 integrase. *J Med Chem* 48(6): 1930-1940.
48. Buolamwini JK, Assefa H (2002) CoMFA and CoMSIA 3D QSAR and docking studies on conformationally-restrained cinnamoyl HIV-1 integrase inhibitors: Exploration of a binding mode at the active site. *J Med Chem* 45(4): 841-852.
49. Artico M, Di Santo R, Costi R, Novellino E, Greco G, et al. (1998) Geometrically and conformationally restrained cinnamoyl-compounds as inhibitors of HIV-1 integrase:

- synthesis, biological evaluation and molecular modeling. *J Med Chem* 41(21): 3948-3960.
50. Fesen MR, Kohn KW, Leteurtre F, Pommier Y (1993) Inhibitors of human immunodeficiency virus integrase, *Proc. Natl. Acad. Sci. USA.* 90(6): 2399-2403.
  51. Sahu KK, Ravichandran V, Jain PK, Sharma S, Mourya VK, et al. (2008) QSAR Analysis of Chicoric Acid Derivatives as HIV-1 Integrase Inhibitors. *Acta Chim Slov* 55: 138-145.
  52. Xu YW, Zhao GS, Shin CG, Zang HC, Lee CK, et al. (2003) Caffeoyl naphthalenesulfonamide derivatives as HIV integrase inhibitors. *Bioorg Med Chem* 11(17): 3589-3593.
  53. Makhija MT, Kulkarni VM (2002) QSAR of HIV-1 integrase inhibitors by genetic function approximation method. *Bioorg Med Chem* 10(12): 1483-1497.
  54. Ma XH, Zhang XY, Tan JJ, Chen WZ, Wang CX (2004) Exploring binding mode for styrylquinoline HIV-1 integrase inhibitors using comparative molecular field analysis and docking studies. *Acta Pharmacol Sin* 25(7): 950-958.
  55. Sharma H, Patil S, Sanchez TW, Neamati N, Schinazi RF (2011) Synthesis, biological evaluation and 3D-QSAR studies of 3-keto salicylic acid chalcones and related amides as novel HIV-1 integrase inhibitors. *Bioorg Med Chem* 19(6): 2030-2045.
  56. DeMelo EB, Ferreira MMC (2009) Multivariate QSAR study of 4,5-dihydropyrimidine carboxamides as HIV-1 integrase inhibitors. *Eur J Med Chem* 44(9): 3577-3583.
  57. Asante-Appiah E, Skalka AM (1997) A metal-induced conformational change and activation of HIV-1 integrase. *J BiolChem* 272(26): 16196-16205.
  58. Bujacz G, Alexandratos J, Wlodewer A, Merkel G, Andrade M, et al. (1997) Binding of different divalent cations to the active site of avian sarcoma virus integrase and their effects on enzymatic activity. *J BiolChem* 272(29): 18161-18168.
  59. Gupta P, Roy R, Garg P (2009) Docking-based 3D-QSAR study of HIV-1 integrase inhibitors. *Eur J Med Chem* 44(11): 4276-4287.
  60. Kaushik S, Gupta SP, Sharma PK, Anwar Z (2011) A QSAR study on some series of HIV-1 integrase inhibitors. *Med Chem* 7(6): 553-560.
  61. Magalhães UD, De Souza AMT, Albuquerque MG, De Brito MA, Cabral LM, et al. (2013) Hologram quantitative structure-activity relationship and comparative molecular field analysis studies within a series of tricyclic phthalimide HIV-1 integrase inhibitors. *Drug Des Develop Ther* 7: 953-961.
  62. Lu P, Wei X, Zhang Y, Fu W (2010) CoMFA and CoMSIA 3D-QSAR studies on quionolone carboxylic acid derivatives inhibitors of HIV-1 integrase. *Eur J Med Chem* 45(8): 3413-3419.
  63. Cheng Z, Zhang Y, Fu W (2010) QSAR study of carboxylic acid derivatives as HIV-1 Integrase inhibitors. *Eur J Med Chem* 45(9): 3970-3980.
  64. Gardelli C, Nizi E, Muraghia E, Crescenzi B, Ferrara M, et al. (2007) Discovery and synthesis of HIV integrase inhibitors: development of potent and orally bioavailable N-methyl pyrimidones. *J Med Chem* 50(20): 4953-4975.
  65. Kaushik S, Gupta SP, Sharma PK, Anwer Z (2011) A QSAR study on a series of N-methyl pyrimidones acting as HIV integrase inhibitors. *Indian J Biochem Biophys* 48: 427-434.
  66. Neamati N, Hong H, Owen JM, Sunder S, Winslow HE, Christensen, et al. (1998) Salicylhydrazine-containing inhibitors of HIV-1 integrase: implication for a selective chelation in the integrase active site. *J Med Chem* 41(17): 3202-3209.
  67. Sreejayan S, Rao MNA (1994) Curcuminoids as potent inhibitors of lipid peroxidation, *J Pharm Pharmacol* 46(12): 1013-1016.
  68. Montterini R, Foresti R, Bassi R, Green CJ (2000) Curcumin, an antioxidant and anti-inflammatory agent, induces heme oxygenase-1 and protects endothelial cells against oxidative stress. *Free Radic Biol Med* 28(8): 1303-1312.
  69. Araujo CC, Leon LL (2001) Biological activities of *Curcuma longa* L. *Mem Inst Oswaldo Cruz* 96(5): 723-728.
  70. Pipier JT, Singhal SS, Salameh MS, Torman RT, Awasthi YC, et al. (1998) Mechanisms of anticarcinogenic properties of curcumin: the effect of curcumin on glutathione linked detoxification enzymes in rat liver. *Int J Biochem Cell Biol* 30(): 445-456.
  71. Elattar TMA, Virji AS (2000) The inhibitory effect of curcumin, genistein, quercetin and cisplatin on the growth of oral cancer cells *in vitro*. *Anticancer Res* 20(3A): 1733-1738.
  72. Pardee AB, Li J, Crumpacker C, Zang L (1994) Treatment of human viral infections. US patent US933470, WO9404139, pp 1-31.
  73. Mazumder A, Neamati N, Sunjay S (1997) Curcumin analogs with altered potencies against HIV-1 integrase as probes for biochemical mechanisms of drug action. *J Med Chem* 40(19): 3057-3063.
  74. Mazumder A, Raghavan K, Weinstein J, Kohn KW, Pommier Y (1995) Inhibition of human immunodeficiency virus type-1 integrase by curcumin. *Biochem Pharmacol* 49(8): 1165-1170.
  75. Artico M, Santo RD, Costi R, Novellino E, Greco G, et al. (1998) Geometrically and conformationally restrained cinnamoyl compounds as inhibitors of HIV-1 integrase: synthesis, biological evaluation, and molecular modeling. *J Med Chem* 41(21): 3948-3960.
  76. Sui Z, Salto R, Li J, Craik C, Montellano PR (1993) Inhibition of the HIV-1 and HIV-2 proteases by curcumin and curcumin boron complexes. *Bioorg Med Chem* 1(6): 415-422.
  77. Vajragupta O, Boonchoong P, Morris GM, Olson JA (2005) Active site binding modes of curcumin in HIV-1 protease and integrase. *Bioorg Med Chem Lett* 15(14): 3364-3368.
  78. Hazuda DJ, Felock P, Witmer M, Wolfe A, Stillmock K, et al. (2000) Inhibitors of strand transfer that prevent integration and inhibit HIV-1 replication in cells. *Science* 287(5453): 646-650.
  79. Yoshinaga TSA, Fujishita T, Fujiwara T (2002) *In vitro* activity of a new HIV-1 integrase inhibitor in clinical development. In 9<sup>th</sup> Conference on Retroviruses and Opportunistic Infections, Seattle, USA.
  80. Pais GCG, Zhang XC, Marchand C, Neamati N, Cowansage K, et al. (2002) Structure activity of 3-aryl-1,3-diketo-containing compounds as HIV-1 integrase inhibitors. *J Med Chem* 45(15): 3184-3194.

81. Marchand C, Zhang XC, Pais GCG, Cowansage K, Neamati N, et al. (2002) Structural determinants for HIV-1 integrase inhibition by beta-diketo acids. *J Biol Chem* 277(15): 12596-12603.
82. Dayam R, Neamati N (2004) Active site binding modes of the beta-diketoacids: a multi-active site approach in HIV-1 integrase inhibitor design. *Bioorg Med Chem* 12(24): 6371-6381.
83. Goldgur Y, Dyda F, Hickman AB, Jenkins TM, Craigie R, et al. (1998) Three new structures of the core domain of HIV-1 integrase: an active site that binds magnesium. *Proc Natl Acad Sci USA* 95(16): 9150-9154.
84. Maignan S, Guilloteau JP, Zhou-Liu Q, Clement-Mella C, Mikol V (1998) Crystal structures of the catalytic domain of HIV-1 integrase free and complexed with its metal cofactor: high level of similarity of the active site with other viral integrases. *J Mol Biol* 282(2): 359-368.
85. Asante-Appiah E, Skalka AMA (1997) A metal-induced conformational change and activation of HIV-1 integrase. *J Biol Chem* 272(26): 16196-16205.
86. Bujacz G, Jaskolski M, Alexandratos J, Wlodawer A, Merkel G, et al. (1996) The catalytic domain of avian sarcoma virus integrase: conformation of the active-site residues in the presence of divalent cations. *Structure* 4(1): 89-96.
87. Yuan H, Parrill AL (2002) QSAR studies of HIV-1 integrase inhibition. *Bioorg Med Chem* 10(12): 4169-4183.
88. Neamati N, Hong H, Sunder S, Milne GWA, Pommier Y (1997) Potent inhibitors of human immunodeficiency virus type 1 integrase: identification of a novel four-point pharmacophore and tetracyclines as novel inhibitors. *Mol Pharmacol* 52(6): 1041-1055.
89. Neamati N, Hong H, Mazumder A, Wang S, Sunder S, et al. (1997) Depsides and depsidones as inhibitors of HIV-1 integrase: discovery of novel inhibitors through 3D database searching. *J Med Chem* 40(6): 942-951.
90. Yuan H, Parrill A (2005) Cluster analysis and three-dimensional QSAR studies of HIV-1 integrase inhibitors. *J Mol Graph Model* 23(4): 317-328.
91. Makhija MT, Kulkarni VM (2001) Molecular electrostatic potentials as input for the alignment of HIV-1 integrase inhibitors in 3D QSAR. *J Comput Aided Mol Des* 15(11): 961-978.
92. Iyer MI, Hopfinger AJ (2007) Treating Chemical Diversity in QSAR Analysis: Modeling Diverse HIV-1 Integrase Inhibitors Using 4D Fingerprints. *J Chem Inf Model* 47(5): 1945-1960.
93. Nunthaboot N, Tonmunpuean S, Parasuk V, Wolschana P, Kokpal S (2006) Three-dimensional quantitative structure-activity relationship studies on diverse structural classes of HIV-1 integrase inhibitors using CoMFA and CoMSIA. *Eur J Med Chem* 41(12): 1359-1372.
94. Nicklaus MC, Neamati N, Hong H, Mazumder A, Sunder S, et al. (1997) HIV-1 Integrase Pharmacophore: Discovery of Inhibitors through Three Dimensional Database Searching. *J Med Chem* 40(6): 920-929.
95. Barreca ML, Rao A, Luca LD, Zappala M, Gurnari C, et al. (2004) Efficient 3D Database Screening for Novel HIV-1 IN Inhibitors. *J Chem Inf Comput Sci* 44(4): 1450-1455.
96. Garg R, Ko GM (2014) In Cancer Causing Vituses and Their Inhibitors. In: Gupta SP (Ed.), CRC Press, Taylor and Francis Group, Florida, USA, pp. 345-406.